Addis Ababa University

Addis Ababa Institution of Technology

African Railway Center of Excellence

Simulation and Control of Wheel Flange Climbing Derailment Using Actuators

A Research report Submitted to the School of Graduate Studies of Addis Ababa University in Partial Fulfillment of the Requirements for the Degree of Masters of Science in Railway Engineering (Rolling stock)

Prepared by: Mensur Birhan (GSR/5177/04)

Advisor: Dr. Eng. Zewudu Abadi

Co-Advisor:Mr. Tolosa Deberie

Nov. 2016

Addis Ababa Ethiopia

APPROVAL PAGE

ADDIS ABABA UNIVERSITY

Addis Ababa Institute of Technology

African Railway Center of Excellence

Title: - Simulation and Control of Wheel Flange Climbing Derailment Using Actuators

Mensur Birhan (GSR/5177/04)

_____	_____	_____
Advisor	Signature	Date
_____	_____	_____
Co-Advisor	Signature	Date
_____	_____	_____
Internal Examiner – 1	Signature	Date
_____	_____	_____
Internal Examiner – 2	Signature	Date
_____	_____	_____
External Examiner	Signature	Date
_____	_____	_____
ARCE Center Head	Signature	Date

DECLARATION

I, the undersigned, declare this thesis work is my original work, has not been presented for a degree in this or any other universities, and all sources of materials used for the thesis work have been fully acknowledged.

Name	Signature	Date of submission
Mensur Birhan Ahmed	_____	_____

Place: Addis Ababa AAIT

This thesis has been submitted for examination with my approval as a university advisor

1. Dr. Eng. Zewdu Abadi	_____	_____
Advisor	Signature	Date
2. Mr. Tolosa Deberie	_____	_____
Co-advisor	Signature	Date

Acknowledgments

First, let me offer my appreciation to Mr. Tolosa Deberie and my advisor and co-advisor, Dr. Ing. Zewudi Abadi. They all provided me with immense support, practical guidance, and abundance of ideas during the whole research work. I relished every moment of the work I had to do for Master of Science project titled Simulation and Control of Wheel Flange Climbing Derailment Using Actuators.

Ethiopian Railway Corporation deserves my appreciation too, for granting me the marvellous opportunity to study at AAIT. I couldn’t have achieved anything worthwhile here without their help.

I would also want to take this opportunity to thank my wife and parents for the unrelenting faith they had on me and their enduring support. In this case, there's nothing I can do to repay my debt, but I can attempt to make them proud. Their assistance and love have been pivotal for my success. There are so many individuals who have supported and assisted me during the past two years that it's difficult to compile a list, but I'm still extremely thankful to them.

Abstract

This research explores how active actuation systems can affect rail vehicle dynamics, using a combined multibody simulation and experimental verification strategy. The research addresses an important issue concerning vehicle-track interaction, particularly large vibrations, instabilities in wheel-rail contact forces, and potential derailment, as each of these factors critically impact ride quality, safety operations, and maintenance costs. The methodology contrasts multibody dynamics modeling with experimental validation of key metrics, such as accelerations of the car body and bogie, wheel-rail contact forces, derailment coefficients, wheel lift, attack angles, and spectral vibration characteristics. The simulation-based evaluation compares system performance with and without active control under various operational conditions. The paper will demonstrate the capability of active control to mitigate harmful rail vehicle dynamics. The findings indicate significant improvements across all assessed measures. Active control leads to a 52% improvement in vertical car body acceleration (from 0.076 m/s^2 to 0.0375 m/s^2) and a 35.7% improvement in lateral acceleration (0.28 m/s^2 to 0.18 m/s^2), markedly improving ride comfort and stability. The wheel-rail contact forces are reduced by 1.3% vertically (73.75 kN to 72.8 kN) and laterally 3.6% (8.9 kN to 8.3 kN), which improves wear characteristics and longevity of components. The derailment coefficient is lower by 4.3% (0.115 to 0.11), improving the safety margin, and wheel lift is lower by 2.1% (375×10^{-6} m to 367×10^{-6} m), facilitating better contact stability. Spectral analysis reveals that active control shifts resonant frequencies down (e.g. from 9.67 Hz to 8.75 Hz) for car body vibrations and simultaneously reduces amplitudes, which signifies that well-targeted vibration suppression is achievable within critical frequency bands. These results give strong support to advance the implementation of active actuation in rail systems, especially in high-speed applications where dynamic performance is important. We showed that active control improves safety, comfort, and maintenance efficiency; furthermore, it also validated both theoretical and experimental models in our study. These results provide a practical basis to use active suspension in future rail vehicles.

Keywords: Active Actuator, vehicle-dynamics, Wheel/rail interaction, Vibration, Derailment coefficient, Multibody -simulation.

Table of Contents

List of Figures

List of Tables

Chapter one

1. Introduction

A serious safety risk in railway systems is wheel flange climbing derailment, which happens when the wheel flange climbs above the rail head and may cause an accident. The goal of this thesis is to improve derailment avoidance techniques by mimicking and manipulating this process with active actuators.

1.1 Background

over two centuries ago, when trains were just being developed, some people feared that the velocity would make the passengers "unable to breath" and that "the passenger would be shaken unconscious by vibrations." But we do know better today. Actually, did you know that there are trains traveling at speeds of over 300 miles per hour (mph)? Apparently, trains have come a long way from their first attempts onto the tracks. Similar to other transportation modes, trains, in their present form, have taken thousands of years to develop[8]/ Railway derailment can result from increased lateral forces, track alignment, or wheel-rail contact instabilities. When the lateral force of a wheel is greater than the vertical load, flange climbs up the rail and is also known as "flange climbing." Active control using actuators minimizes the risk of derailment[9].

Brief History of Railway

Railways have been instrumental in the growth of civilizations across the globe. Railways have traveled a long distance from the ancient Greek trackways to the futuristic Hyperloop of today as illustrated in Figure 1-1.

Figure 1- 1an Ancient Greek Roadway that carried ship on land[1]

This article-traces the history of train technology, from its rudimentary forms, innovations during the Industrial Revolution, and innovations to modern train systems. The earliest rail transport was utilized in ancient Greece around 600 B.C. The Greeks made grooves in paved limestone roads for transporting boats across the Isthmus of Corinth. This facilitated the movement of wheeled vehicles. When the Romans conquered Greece in 146 B.C.,

Figure 1- 2 loaded coal Train wagons[2]

these early railways fell into disuse and disappeared for over 1,400 years.[2]Its successful operation led other engineers to improve upon his design

Re-emergence in the 16th Century: Wagon ways

Railways came back in the 16th century. Wagon ways, the predecessors of today's trains, were spotted in Germany in the 1550s. They were merely wooden rails upon which horse-drawn wagons moved more efficiently than on earth roads. Wooden rails were substituted by iron by the 1770s, and tramways became widespread in Europe.[2]

The Industrial Revolution and the Steam Engine

This article traces the history of train technology, from its ancient beginnings, Industrial Revolution innovations, and innovations up to modern train systems. Ancient Greece,

around 600 B.C., witnessed the initial rail-based transportation. The Greeks made grooves in paved limestone roads to transport boats over the Isthmus of Corinth. This facilitated The Industrial Revolution established the groundwork for complex railway systems. The steam engine changed innovation. In 1803, Samuel Homfray funded a steam-powered cart to take the place of horse-drawn carts. In 1804, Richard Trevithick invented the first tramway locomotive powered by a steam engine.

Figure 1- 3Richard Trevitthick built the first steam engine[2]

It was able to carry 10 tons of iron, 70 men, and five wagons on a nine-mile ride.[8]George Stephenson developed this technology further in the early 19th century. In 1821, he constructed the first steam locomotive for the Stockton & Darlington Railway Line. His 1829 model, the Rocket, became the benchmark for steam engines for 150 years.[9] to come the wheeled transportation. When the Romans conquered Greece in 146 B.C.,

First Commercial Steam Locomotive:

The Salamanca, designed and built by Matthew Murray, was the first steam locomotive to be commercially successful, predating Stephenson's Rocket by 17 years.

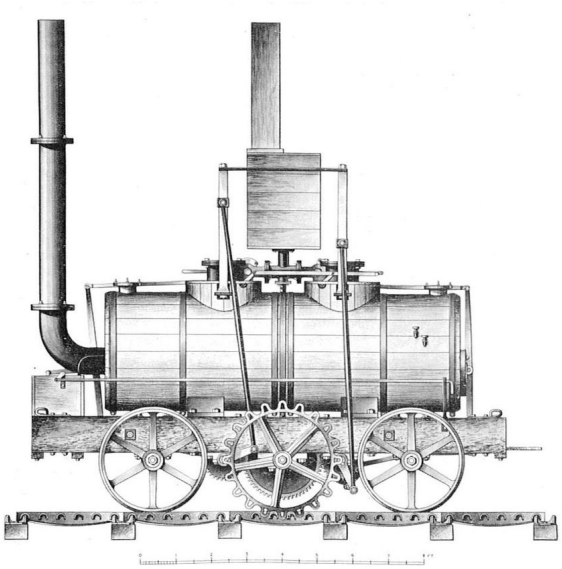

Figure 1- 4The Salamanca locomotive[1]

The History of African Railroads

The first Europeans to move through Africa by rail were missionaries. Two French priests laid a narrow-gauge railway track in French Congo (now Republic of Congo) from Brazzaville to Pointe Noire in 1878 where they planned to open a mission station. The linewas never completed because the priests learned that they could not maintain maintenance fees or pay their workers; they abandoned it after it had existed for only three years[10]

At the same time, British interest in constructing railways across Africa started when Cecil Rhodes became prime minister of Cape Colony in 1890. He envisioned linking various sections of his huge territory with trains–but only after a series of failed attempts did he succeed at making this a reality with his Cape Town-Pretoria line (later called Table Bay Railway). But profitable this venture was though, it did not actually stimulate much more growth until 1908 when King Leopold II announced plans for what later came to be known as Trans-African Railway (TAR). This massive project had the aim of linking it all together within a single system but was too complicated due to its enormous proportions – costing over $100 million USD per mile to build alone![11]

When did Railway start in Ethiopia?

Ethiopia's first railroad was the 780km metre gauge line from the capital, Addis Ababa, to the port of Djibouti in the country of that name. The first section, between Djibouti (then in French Somaliland) and Dire Dawa in Ethiopia (then Abyssinia), opened in 1901,

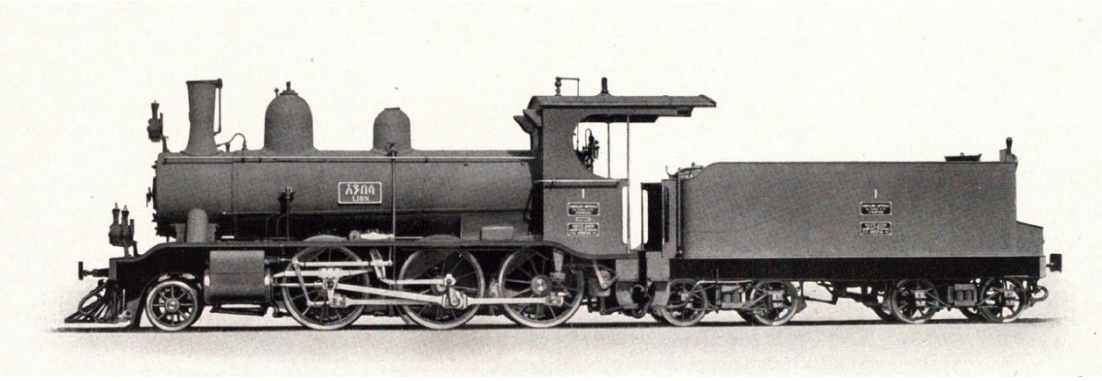

Figure 1- 5in 1899, the very first steam locomotive of the railway[12]

but further construction was stopped by bankruptcy of the original railway company, and the line to Addis Ababa was not completed until 1917. On the independence of Djibouti ownership of the line was taken over by a new company jointly owned by the two governments. However, in the late 20th / early 21st centuries, the line was allowed to deteriorate and run down, the service became infrequent, and the line ultimately closed. A new 760km standard (1435mm) gauge electrified railway opened from Addis Ababa to Djibouti in 2016, replacing the metre gauge railway. About 660km of this line is in Ethiopia.[12] In 2023, a 392km branch of the Addis Ababa to Djibouti line was opened from a junction at Awash to Hara Gebeya. A further 260km from Hara Gebaya to Mek'ele is under construction. Addis Ababa also has a modern tramway system, 32km long, opened in 2015.[13]

Challenges Facing in The Railway Industry Especial in Derailment Case

Train Derailment Statistics: Over 1,000 Total Train Derailments The United States in 2022 experienced an impressive 1,164 train derailments, thereby highlighting the daunting challenge facing the rail industry in offering safe and reliable transport throughout the country][14]

1.2 Problem statement

Train derailments present serious safety risks that can lead to accidents, infrastructure damage, as well as financial losses. Wheel flange climbing, occurring when the wheel flange rises over the rail head due to dynamic instabilities, misalignment, or excessive lateral force, is a critical failure mode among derailment devices. In severe situations (e.g., sharp curve optimised wheel profiles, and track maintenance may not be sufficient to prevent derailment. Active control through actuators is a promising solution by introducing dynamic changes in wheel- rail forces to prevent flange climbing. Successful implementation of these systems, however, requires accurate simulation models of wheel-rail contact under derailment. Strong control algorithms with the capability of performing real-time force compensation. Validation of actuator performance in literature and simulation.

1.3 Research Questions

- How do different wheel-rail contact conditions influence flange climb derailment?
- What type of actuator (hydraulic, electromechanical, etc.) is most effective for real-time derailment prevention?
- Which control algorithm provides the best trade-off between response time, stability, and energy efficiency?
- Can an actuator-based system outperform traditional passive solutions in preventing flange climbing?

1.4 Objective

1.4.1 General Objective

The main objective of this study is to design an active control system using actuators with the aid of computational simulation and literature review validation, thus improving railway safety and operation reliability.

1.4.2 Specific Objectives

- Determine the Influence of car body and bogie acceleration on derailment of the Vehicle
- Reduce the Influence of wheel/rail contact force on derailment of the Vehicle
- Analyse the effect of car body and bogie acceleration on derailment of the Vehicle

- Investigate the significance of coefficient of derailment on the system dynamic performance.
- Determinate the wheel raise effect during the wheel/rail contact.
- The variation of roll angle (attack) angle effect on vehicle derailment.
- Introduced the power spectral density (PSD) for Carboy and bogie on derailment of the Vehicle

1.5 Research significance

The significance of the study is crucial to improve railroad safety and operating effectiveness. The aim of this study is to create an anticipatory approach to avoiding the most dangerous derailment mechanism, flange climbing, by addressing the main derailment drivers such as these high lateral forces, unfavourable attack angles, and unstable creep forces. Conventional passive solutions, i.e., friction control or wheel profile adjustment, tend to respond too late to changes in track conditions. Actuator-controlled systems, on the other hand, are capable of stabilizing wheel-rail interaction in real time before derailment can take place. Through less wear on wheel and rail, the method lessens maintenance expenditure simultaneously improving safety of freight and passengers. Furthermore, the research develops more advanced intelligent rail systems to benefit upcoming autonomous trains in needing self-correcting systems for high speed operation and operating close to tight bends. This study fills the gap between theoretical models and practical application by confirming performance based on quantifiable measures (e.g., maintenance of attack angle control, decreasing L/V ratio), and is thus a practical guide for policymakers and railway engineers. Finally, the study brings derailment prevention technology into consideration for modern rail systems that are more efficient in terms of energy, cost-effective, and more reliable.

1.6 Scope and limitation of research

Important parameters such as lateral forces, attack angles, and creep forces at wheel-rail contact are the object of this work, which imitates and controls actively wheel flange climbing derailment using actuators. For reduction of the danger of derailments, the research will include actuator performance testing, design of real-time control algorithms, and numerical modelling of derailment dynamics and SIMPACK SOFTWARE based simulation and literature review will be employed for verification purposes; operational situations will include track irregularities,

sudden curves, and multiple speeds. But the study has a number of limitations. The study investigates only flange climbing derailment; it does not investigate roll-over or gauge widening, two other derailment processes. Full-scale application is unlikely in the near future due to practical limitations like actuator power demands and space for mounting on actual trains. The simulations use simplified contact models, which are not necessarily accurate for extreme conditions like dirty railroads or bad weather. Moreover, although field verification of the robustness of control algorithms is established, more field testing must ensure long-term reliability under constant operating stress. These field limitations illustrate just how much work lies ahead to close the gap between theoretical solutions and real application.

1.7 Research methodology

Using advanced simulation techniques and theoretical validation, this study implements a rigorous computational methodology to investigate the use of actuator-based systems to manage wheel flange climbing derailment. The three closely interdependent stages of study methodology numerical modelling, simulation analysis, and literature-based validation—are all carried out using SIMPACK software to establish an advanced multibody dynamics model that comprehensively describes the intricate wheel-rail interaction dynamics forms the nucleus of the investigation. Crucial details of this model are accurate models of suspension system behaviour, nonlinear contact mechanics based on Kalker's theory, and realistic wheel and rail profiles. The dynamic response characteristics and operating conditions of the actuator systems are accounted for through mathematical simulation thereof as force elements in the simulator environment. curve at various speeds, are rigorously analysed for the simulation analysis phase. In-depth details regarding wheel set kinematics, risk of derailment indicators, and wheel-rail contact forces are provided by these models and their efficiency in reducing flange climbing is tested. In-depth parametric analyses to improve control settings and system performance assessment based on varying operating conditions are enabled using the simulation environment. Simulation results are validated against a data from similar studies published in peer-reviewed journals are compared against simulation results. For analysis of the robustness of the control system to parameter variations like track stiffness, wheel-rail friction coefficient, and actuator response characteristics, the approach encompasses sensitivity analysis. For measurement of performance parameters like derailment risk reduction, actuator force demands, and system response times,

statistical analysis techniques are applied to simulation results. The aim of the entire exercise is to demonstrate, through theoretical merit and to acceptable engineering standards, the feasibility and efficacy of preventing actuator-based flange climb.

Chapter 2. literature review

2.1. Introduction

Wheel flange climbing derailment remains an important safety concern in rail transit systems, which occurs under the condition of high lateral forces causing the wheel flange to climb over the rail head. Traditional passive solutions such as optimized wheel profiles and friction management have their own limitations during dynamic operation. Advanced active control systems, particularly those employing actuators, are promising countermeasures to preactively minimize the dangers of derailment in real time.

2.2. Wheel-Rail contact mechanics and wear

Adhesion is the chief reason behind which trains travel securely, economically, and with certainty on a rail network. While accelerating, braking, and coming to stop ensuring an optimum state of adhesive force is an essential subject matter to be dealt withWheel rail contact is also a critical issue in railways because it determines the tractive or braking force that could be applied to minimize slip.[15] As it is known, contacting surfaces are both metals, and there is a very small area of contact between the components (wheel and rail) compared to their surface area, imposing a tremendous amount of stress on the surfaces at the contacting interface (Contact patch). In addition, since there are no steering mechanisms for train wheels, they accommodate curving by performing a wheel slide on the rail causing even higher stress at the interface. The main intention here is therefore to determine the stress, deformation and shape of the contact patch.

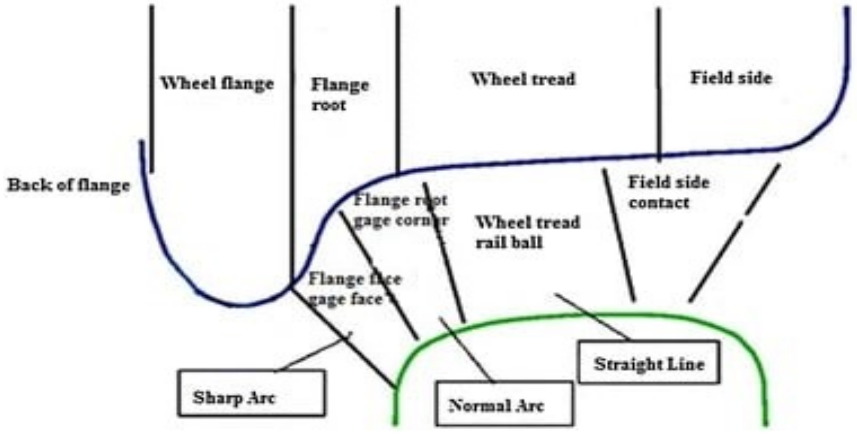

Figure 2- 1Contact surfaces description[3]

The contact mechanics is highly influenced by the following important factors[15]

- Number of bodies under contact
- The geometry of the bodies
- The material property of the bodies
- Deformation mode of the bodies
- Contact force imposed between the bodies
- Type of relative motion between them (static, sliding, rolling)
- The velocity of the relative motion

In general, there are two types of contact between wheel and rail, i.e., thread contact and flange contact, and a combination of them at some point. Thread contact denotes contact between the wheel and rail at the thread portion of the wheel and rail and Flange contact where the contact occurs in the flange section, as shown in the Figure above.The general contact theory was developed by Hertz in 1882. Based on his fringes experiment, he proposed the contact between two non-conformal revolving on one another as elliptical shape and normal pressure distribution is taken to be semi-ellipsoid by taking the following assumptions during the process [15]

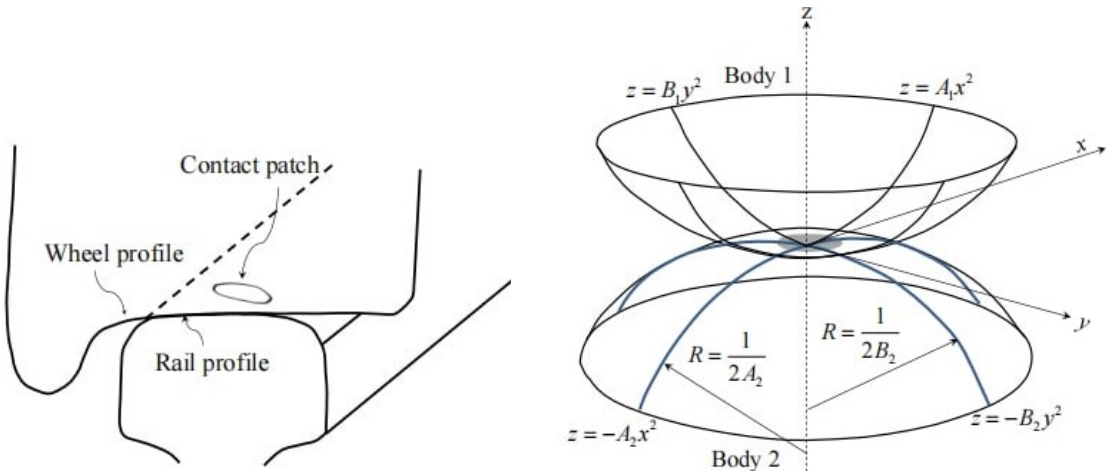

Figure 2- 2Contact patch representation[4]

- Materials in contact are homogeneous and yield stress is not exceeded
- The effect of surface roughness is negligible
- The normal load causes contact stress to tangent contact plane/ no tangential force

- The contact area is very small compared to the whole dimension of the bodies

In the following contact mechanics analysis's, R_w and R_r are the radius of curvature of wheel thread and rail head at the contact point, r is radius of wheel, N is the normal force acting on the contact area, a and b are the major and minor axis semi-lengths given by [5]

$$(a/m)^3 = (b/n)^3 = 3N(1-v^2)/E(1/r + 1/R_r - 1/R_w) \quad Eq\ 2\text{-}1$$

$$cos\ \beta = (1/r + 1/R_r - 1/R_w)/(1/r - 1/R_r + 1/R_w) \quad Eq\ 2\text{-}2$$

Where: E = Youngs modulus v = Poisson Ratio

m and n = hertzian parameters tabulated in terms of hertzian contact constant beta

Table 2- 1Hertzian contact coefficients (m and n)

(^{0})	m	n	(^{0})	M	n
0		0	50	1.754	0.641
1	36.89	0.131	55	1.611	0.678
10	6.612	0.319	60	1.486	0.717
20	3.778	0.408	65	1.378	0.759
25	3.152	0.456	70	1.284	0.802
30	2.731	0.493	75	1.202	0.846
35	2.397	0.530	80	1.128	0.893
40	2.136	0.567	85	1.061	0.944
45	1.926	0.604	90	1.000	1.000

Using the above analysis, the value of the elliptical contact patch's major and minor axis length (2a and 2b) can be found.

The maximum normal pressure and shear stress along the contact patch for Hertzian contact and railhead respectively, could also be found as follows:

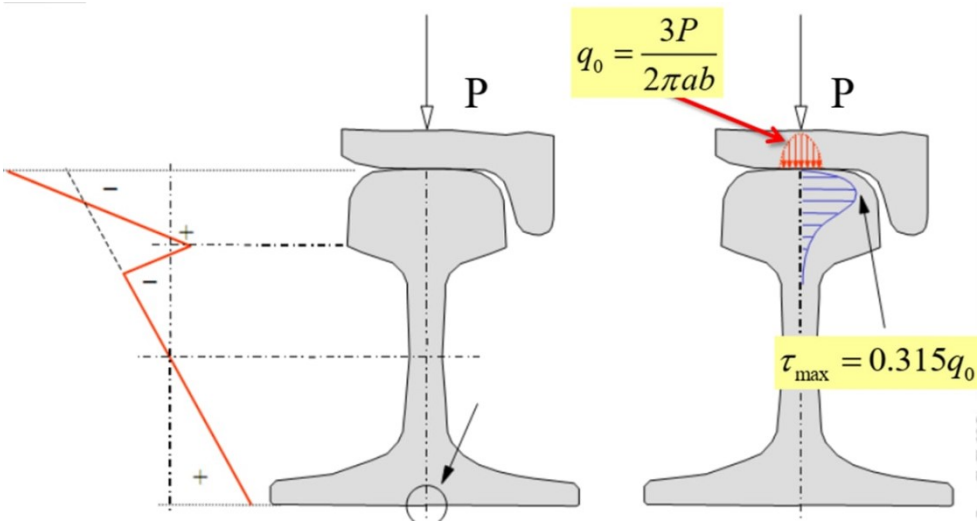

Figure 2- 3Maximum normal and shear pressure acting on the contact patch[5]

But the above assumptions don't always hold true, especially in contact conditions at rail gauge, wheel flange, and worn profile wheels. Many other non-Hertzian or modified Hertzian contact models are found in different literatures, which account for these factors in the contact mechanics.

When a longitudinal force is applied to wheels, a deviation from rolling motion occurs, i.e., slippage or Creepage. A deviation in relative velocity in the longitudinal direction between the wheel and rail concerning the forward speed is called longitudinal creepage. On the other hand, Lateral creepage is the incremental relative lateral velocity concerning wheel and rail about the forward speed. Finally, spin is the relative angular motion between the wheel and rail about the normal contact axis. Mathematically, these are expressed as [5]

$$\gamma_1 = \frac{(V_x^w - V_x^r)}{V} \qquad \gamma_2 = \frac{(V_y^w - V_y^r)}{V} \qquad \omega_3 = \frac{(\Omega_z^w - \Omega_z^r)}{V} \qquad \textit{Eq 2-3}$$

Where: γ_1 = Longitudinal creepage, γ_2 = Lateral creepage, ω_3 = Spin creepage, and V and Ω represent translational and angular velocities of wheel or rail (w or r as superscript).

For the small value of creepages and spin, adhesion prevails along the whole contact patch. As shown in the following expressions, creep forces have a linear relationship with creepage.

$T_1 = -f_{11}\gamma_1 \quad T_2 = -f_{22}\gamma_2 - f_{23}\omega_3\, M_3 = f_{23}\gamma_2 - f_{33}\omega_3 Eq\ 2\text{-}4$

Where: T_1, T_2 and M_3 are longitudinal, lateral and spin creep forces, respectively

The constants f_{ij} were analyzed by Kalker as follows:

$$f_{11} = Gc^2C_{11} \qquad f_{22} = Gc^2C_{22} \qquad f_{23} = Gc^3C_{23} \qquad Eq\ 2\text{-}5$$

Where: c^2 = ab, and G = Elastic modulus of rigidity and C_{ij} can be found from Appendix 3. Taking f_{11} and f_{22} as equal is a useful approximation during analysis [5]. For an arbitrary creepage condition, Kalker provided a faster approach in the computer program known as FASTSIM and if flexibility in the contact area is to be isotropic, the following relations is a rearrangement of the f_{ij} factors for the small creepage case.

$$f_1 = 8a/3C_{11}G \qquad f_2 = 8a/3C_{22}G \qquad f_3 = \pi a\sqrt{a/b}/4C_{23}G\ Eq\ 2\text{-}6$$

For other complex non-Hertzian contact mechanics conditions, different researchers proposed other methodologies to analyze the real scenario under consideration. For example, a faster and more reliable method of contact calculation was proposed in [16]and [17]based on semi-elliptical pressure distribution in the direction of rolling and curved contact surface approaches, respectively.

Considering the vehicle dynamics of the wheelsets and wheel-rail geometry, the velocity components of the wheels are given by [5]

Wheel Related

$$V_{1l}{}^{w} = \Omega r_l + l\dot{\psi} \qquad Eq\ 2\text{-}7$$

$$V_{2r}{}^{w} = \left(\dot{u}_y^* + \Omega r_r\psi\right)sec\ \delta_r \qquad Eq\ 2\text{-}9$$

$$V_{2l}{}^{w} = \left(\dot{u}_y^* + \Omega r_l\psi\right)sec\ \delta_l \qquad Eq\ 2\text{-}1$$

$$\Omega_{3r}{}^{w} = \Omega sin\ \delta_r + \dot{\psi}cos\ \delta_r \qquad Eq\ 2\text{-}2$$

Rail related

$$V_{1r}{}^{r} = -V\left(1 - \frac{l}{R_0}\right) \qquad Eq\ 2\text{-}8$$

$$V_{1l}^{r} = -V\left(l + \frac{l}{R_0}\right) \qquad Eq\ 2\text{-}10$$

$$V_{2r}^{r} = 0,\ V_{2l}{}^{r} = 0 \qquad Eq\ 2\text{-}12$$

$$\Omega_{3r}^{r} = -\frac{V\ cos\ \delta_r}{R_0} \qquad Eq\ 2\text{-}14$$

$$\Omega_{3l}{}^{w} = -\Omega sin\ \delta_l + \dot{\psi} cos\ \delta_l \qquad \textit{Eq 2-15}$$

$$\Omega_{3l}^{r} = -\frac{V\ cos\ \delta_l}{R_0} \qquad \textit{Eq 2-16}$$

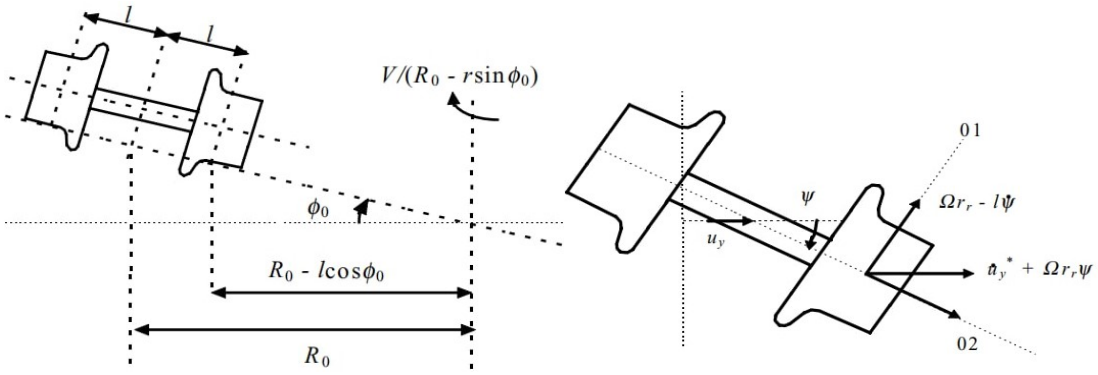

Figure 2- 4Velocity components of wheel and wheelsets [5]

Based on this analysis as the previous case of a single wheel, the wheelset creep forces and creepages for small creepage are calculated as:

Creepage

$$\gamma_{1r} = \frac{\Omega r_r}{V} + 1 - \frac{l\dot{\psi}}{V} - \frac{l}{R_0} \qquad \textit{Eq 2-3}$$

$$\gamma_{1l} = \frac{\Omega r_l}{V} + 1 + \frac{l\dot{\psi}}{V} + \frac{l}{R_0} \qquad \textit{Eq 2-5}$$

$$\gamma_{2r} = \left(\dot{u}_y^* + \Omega r_r \psi\right)\frac{sec\ \delta_l}{V} \qquad \textit{2-21}$$

$$\gamma_{2l} = \left(\dot{u}_y^* + \Omega r_l \psi\right)\frac{sec\ \delta_l}{V} \qquad \textit{Eq 2-6}$$

Creep Forces

$$T_{xr} = T_{lr} \qquad \textit{Eq 2-4}$$

$$T_{yr} = T_{2r} cos\ \delta_r + T_{3r} sin\ \delta_r \qquad \textit{Eq2-20}$$

$$T_{zr} = T_{3r} cos\ \delta_r - T_{2r} sin\ \delta_r \qquad \textit{Eq2-22}$$

$$T_{xl} = T_{ll} \qquad \textit{Eq 2-7}$$

$$\omega_{3r} = (\frac{\Omega}{V})sin\ \delta_r + (\frac{\dot{\psi}}{V})cos\ \delta_r + \frac{cos\,\delta_r}{R_0} \qquad \textit{Eq 2-8}$$

$$T_{yl} = T_{2l}cos\ \delta_l - T_{3l}sin\ \delta_l \qquad \textit{Eq2-9}$$

$$\omega_{3l} = -(\frac{\Omega}{V})sin\ \delta_l + (\frac{\dot{\psi}}{V})cos\ \delta_l + \frac{cos\,\delta_l}{R_0} \qquad \textit{Eq 2-10}$$

$$T_{zl} = T_{3l}cos\ \delta_l + T_{2l}sin\ \delta_l \qquad \textit{Eq 2-11}$$

The final resultant creep forces are found by the following relation based on summation of forces along the direction of application of forces:

$$T_x = T_{xr} + T_{xl} \qquad \textit{Eq 2-12}$$

$$T_y = T_{yr} + T_{yl} \qquad \textit{Eq 2-13}$$

$$T_z = T_{zr} + T_{zl} \qquad \textit{Eq 2-14}$$

$$M_x = T_{zr}l - T_{zl}l - T_{yr}r_r - T_{yl}r_l \qquad \textit{Eq 2-15}$$

$$M_y = \left(T_{xr} + T_{yr}\psi - T_{zr}\psi tan\ \delta_r\right)r_r + \left(T_{xl} + T_{yl}\psi + T_{zl}\psi tan\ \delta_l\right)r_l \qquad \textit{Eq 2-16}$$

$$M_z = T_{xl}l - T_{xy}l \qquad \textit{Eq2-17}$$

2.3. Vehicle Dynamics

2.3.1 Longitudinal Dynamics

The longitudinal dynamic behavior is expressed in terms of combination of differential equations by considering each wagon (MC_1, MC_2 and TP) as a single mass connected by couplers.

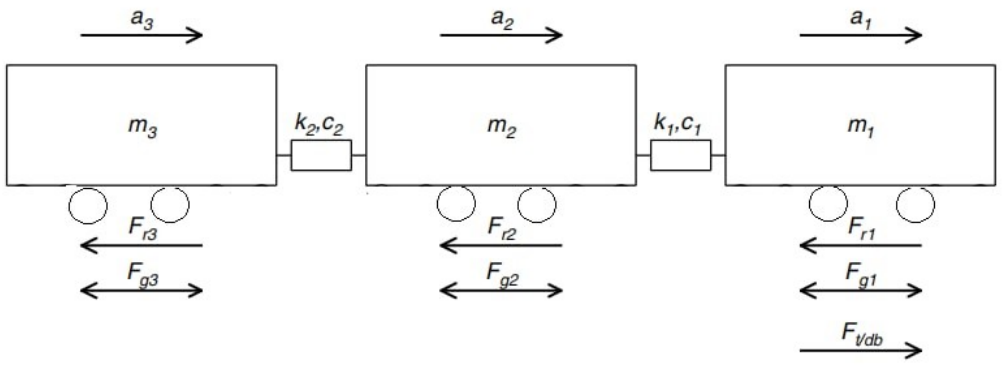

Figure 2- 5Longitudinal dynamics of Train[6]

The longitudinal equation of motion for the i^{th} wagon is given by:

$$m_i a_i + c_{i-1}(v_i - v_{i-1}) + c_i(v_i - v_{i+1}) + k_{i-1}(x_i - x_{i-1}) + k_i(x_i - x_{i+1}) = F_{t/dbi} - F_{ri} - F_{gi}$$

Eq2-18

Where, m_i = mass, a_i = acceleration, v_i = speed, x_i = distance travel, C_i = coupler damping of i^{th} wagon, $F_{t/db}$ = force from locomotive (tractive and braking), F_r = sum of resistances including propulsion, curve, and braking related resistances and F_g= gravitational force due to grade difference.

Since we don't have a locomotive in our case, the $F_{t/db}$ is power supplied for each motored bogie (MC) and zero for TP, while the rest of them will be accounted based on the conditions. Once the system of equations is arranged in the above way, they are collected in terms of the following expression for convenience of calculation.

$$M\ddot{X}(t) + CX(t) + KX(t) = f(t) \qquad \text{In time domain}$$

$$MS^2 + CS + K = \frac{F(S)}{X(S)} \qquad \text{In frequency domain}$$

Analyzing the above equation in a numerical analysis algorithm, state-space method, or other ODE analysis methods will give the system variables of the longitudinal dynamic behavior of each component.

2.3.2 Lateral Dynamics

Considering the lateral dynamics, we have the lateral distance expressed in terms of the conicity and radius of curvature as:

$$\text{OAB} = \text{OCD}$$

$$(r_0 - \lambda y)/(R - l) = (r_0 + \lambda y)/(R + l)$$

$$y = r_0 l/R\lambda$$

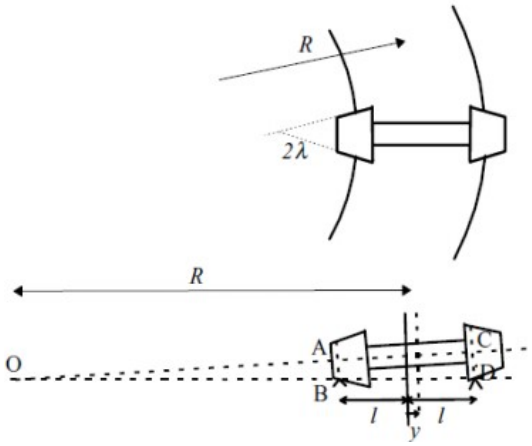

Figure 2- 6Lateral position of wheelset[6]

By taking the components contributing to the lateral motion of the wheelset, assuming a small stiffens of lateral and yaw springs with small displacement and conicity and using summation of forces and yaw torque in the lateral direction with final simplification gives us the following governing equation for the lateral motion of the wheelset.

$$m\ddot{y} + \frac{2f_{22}\dot{y}}{V} + K_y y - 2f_{22}\psi + \left(\frac{2f_{23}}{V} - \frac{I_y \kappa V}{r_0 l}\right)\dot{\psi} = Q_y \qquad \textit{Eq 2-19}$$

$$I_z\ddot{\psi} + \frac{2f_{11}\lambda_0 l y}{r_0} - \left(\frac{2f_{23}}{V} - \frac{I_y \delta_0 V}{r_0}\right)\dot{y} + 2f_{11}l^2\frac{\dot{\psi}}{V} + K_\psi \psi = Q_\psi \qquad \textit{Eq 2-20}$$

Where:

$$Q_y = -\frac{mV^2}{R_o} + mg\phi_0 + \frac{\delta_0 I_y V^2}{R_0 r_o} + 2f_{23}/R_0 \qquad \textit{Eq 2-21}$$

$$K_y = k_y + \left(\frac{2N_0\varepsilon_0^*}{l}\right)\left(1 - \frac{f_{23}}{N_0 r_0}\right) \qquad \textit{Eq 2-22}$$

$$Q_\psi = \frac{I_y V \dot{\phi}_0}{r_0} - I_z V \frac{d}{dt} R_0 - \frac{2 f_{11} l^2}{R_0} \qquad \textit{Eq 2-23}$$

$$K_\psi = k_\psi + 2N_0 l(-\delta_0 + f_{23}/N_0 l) \qquad \textit{Eq 2-24}$$

$$\varepsilon_0^* = l\left(1 + \frac{R_r \delta_0}{l}\right)/(R_w - R_r)\left(1 - \frac{r_0 \delta_0}{l}\right) \qquad \textit{Eq 2-25}$$

Solving the above equation in the appropriate numerical tool gives the necessary system variables to define the lateral motion of the wheelset.

2.3.3 Vertical Dynamics

In the vertical dynamic analysis, the important factors to consider are suspensions (primary and secondary), masses, springs, and dampers, irregularities of rails and external forces applied on them. First the system is modeled as a spring, mass and damper system as shown below.

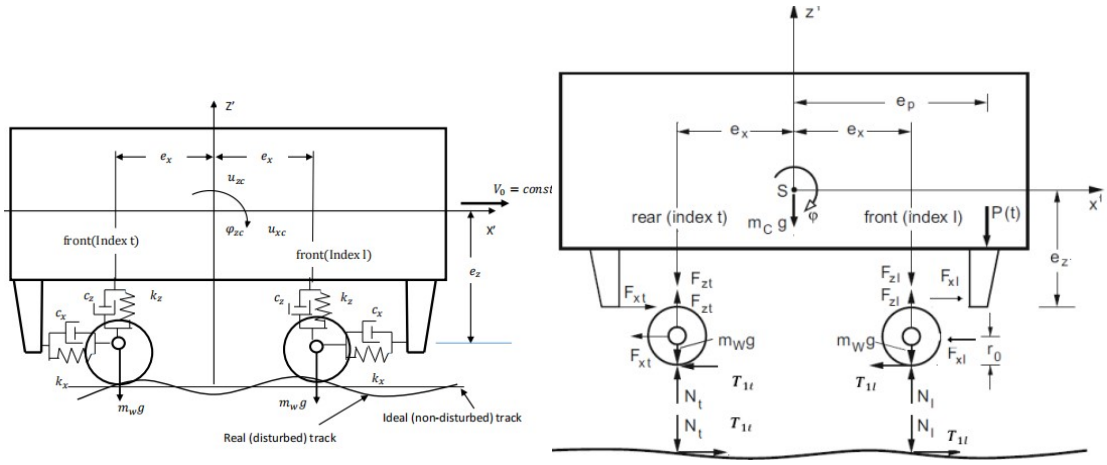

Figure 2- 7Free body model of Train using spring, mass, and damper system[6]

Based on the free body diagram, the equilibrium of forces on the Car body and the two wheels is done, and the equation of motion extracted by applying the sum of force and moment on each body and making the necessary arrangements gives the following general expression, which can be solved using state space, Eigenvalue, numerical method or other ODE solving methods to get the system variables.

$$M\ddot{X} + CX + KX = F \qquad \text{Eq 2-26}$$

Where:

$$\mathrm{M} = \begin{bmatrix} m_{cb} & 0 & 0 & 0 & 0 \\ 0 & m_{cb} & 0 & 0 & 0 \\ 0 & 0 & I_{cb} & 0 & 0 \\ 0 & 0 & 0 & m_w + \frac{I_w}{r_0^2} & 0 \\ 0 & 0 & 0 & m_w + \frac{I_w}{r_0^2} & \end{bmatrix}, \quad \mathrm{C} = \begin{bmatrix} 2c_x & 0 & -2c_x e_z - c_x & -c_x & \\ 0 & 2c_z & 0 & 0 & \\ -2c_x e_Z & 0 & 2c_x e_z^2 + 2c_z e_x^2 & c_x e_z & c_x e_z \\ -c_x & 0 & c_x e_z & c_x & 0 \\ -c_x & 0 & c_x e_z & 0 & c_x \end{bmatrix},$$

$$\mathrm{X} = \begin{Bmatrix} u_{xcb} \\ u_{zcb} \\ \varphi \\ u_{xl} \\ u_{xt} \end{Bmatrix},$$

$$\mathrm{K} = \begin{bmatrix} 2k_x & 0 & & -2k_x e_z & -k_x & -k_x \\ 0 & 2k_z & 0 & 0 & 0 & \\ -2k_x e_z & 0 & 2k_x e_z^2 + 2k_z e_x^2 & k_x e_z & k_x e_z & \\ -k_x & 0 & k_x e_z & k_x & 0 & \\ -k_x & 0 & 0 & k_x e_z & 0 & k_x \end{bmatrix}$$

$$\mathrm{F} = \begin{Bmatrix} 0 \\ m_{cb} g - P(t) + k_z(z_l + z_t) + c_z(\dot{z}_l + \dot{z}_t) \\ P(t)e_p - k_z e_x(z_l - z_t) - c_z e_x(\dot{z}_l - \dot{z}_t) \\ 0 \\ 0 \end{Bmatrix}$$

2.4. Stability and Safety

2.4.1. Nadal's Formula for Safety Criteria

The derailment of wheels from the rail is one of the most devastating failures that could occur in a railway system. Derailment is a process by which the lateral force imposed on the wheel pushes it against the rail at the contact patch, raising the wheel way above the rail gauge, resulting in wheel climbing and, if further kept, derailment. To avoid this phenomenon, safety criteria are the device to quantify it by different publications. These include Weinstock axle-sum L/V criteria, High-speed passenger limit criteria (US), L/V time duration criterion (Japan), and Nadal's single-wheel L/V limit criterion [6]From the above, Nadal and Weinstock criteria are related to L/V ratio limits, while the rest are related to the time and distance exceeding limits of

L/V. The Nadal's safety criterion is proposed for French railways based on a subsequent flange contact due to excess lateral force and it is expressed as follows.

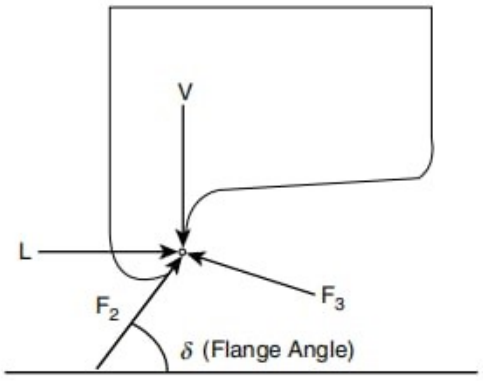

Figure 2- 8Vertical and lateral force application at contact patch [6]

$$\frac{L}{V} = \frac{\tan\,\delta - \mu}{1 + \mu \tan\,\delta} \qquad \text{Eq 2-44}$$

Where: L = Lateral force, V = Vertical force, μ = friction coefficient and δ = flange angle

According to the safety criteria, the value L/V shall not exceed value of 0.8 for avoiding wheel climbing during operation of the trains.

2.4.2.Comfort

For general comfort conditions according to the UIC approach takes the following expression for ride quality computation [6]

$$N_{MV} = 6\sqrt{(a_{XP95})^2 + (a_{YP95})^2 + (a_{ZP95})^2} \qquad \text{Eq 2-45}$$

Where: N_{MV} = Ride Quality, a_{xp} = acceleration in the longitudinal direction, a_{yp} = acceleration in the lateral direction, a_{zp} = acceleration in the vertical direction.

The maximum peak acceleration that could be achieved in all directions is estimated at.3g = 2.943m/s^2 by taking 30% adhesion at most [6]. Further, for N<1 = very comfortable, 1<N<2 = Comfortable, 2<N<4 = medium comfort, 4<N<5 = Uncomfortable, and N>5 = Very uncomfortable conditions hold true. These values are described as ride index in the following analysis and the best comfort condition below

2.4.3.Active Steering Control Strategy

When the Railway Vehicle run on the curved section, attack angle between the Wheel and Rail are generated as shown in the Figure 2-9 . Due to the lack of Steering function of the wheel[18] This causes unnecessary Force in the driving directions and the Lateral direction of the Wheel, which the major cuasing wear of the wheels and Rails and the generation of noise.

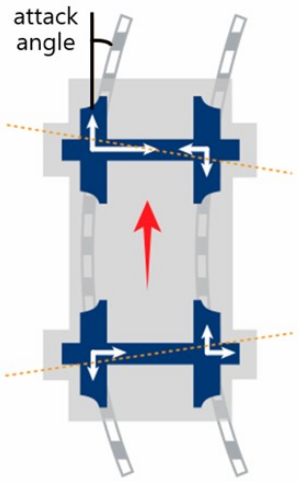

Figure 2- 9Wheelset alignment on a curve [18]

When a conventional Railway Vehicle run on the Curve, in order for the railway vehicle smoothly run the curve section, the angle of attack becomes “0” if the wheelset is aligned with the center of curvature as shown in Figure 2-10using active Figure 2-9 . Wheelset alignment of a conventional railway vehicle when running on curved section. steering control technology. At this time, this geometric position is called the radial steering position.

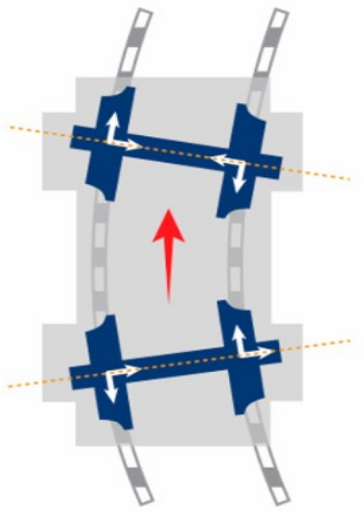

Figure 2- 10Wheelset alignment with active steering [18]

Figure 2-10. shows the geometrical relationship between the body and the bogies, assuming the vehicle is in the Radial Steering position in the curve section. In Figure 2-11 the angle (2 δ) formed between two wheelsets is called steering angle, and the angle (θ) at which the bogie is rotated with respectto the vehicle body is called the bogie anglethe bogie angles of the front and the rear Bogies are the same. At this time, from geometrical relationship of Figure 2-11. The target value for wheelset steering angle and bogies angle for the idea of wheelset steering in the curve section of radius R are derived as shown in Equations (1) and (2)[19, 20]

$$2\delta = 2d/R \qquad \text{Equation 1}$$

$$\theta = L/V \qquad \text{Equation 2}$$

Where,

2δ= steering angle(rad)

R= Radius of Curve(m)

2d= wheelbase(m)

L: semi-spacing of distance between bogie center distance(m)

θ: bogie angle between body and bogie(rad)

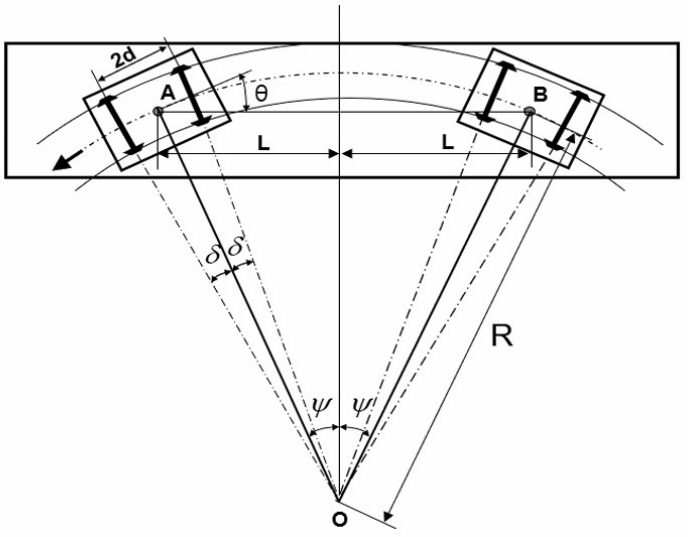

Figure 2- 11Radial steering position[21]

Whenarailwayvehicle is run on a curved section as above, it can ideally pass through the curve if it is located in a radial steering position. In other words, if steering control is performed by calculating the target steering angle by applying Equation (1), the railway vehicle will be located in the radial steering position. In order to apply Equation (1), information on the radius of the curved section passing through is required. Previously, a method of pre-input of the curve information according to the position into the controller was applied, but it was ineffcient. In this paper, the method ofestimating the radius of curvature in real time developed by the author was used, and this method of estimating of the radius of curvature experimentally verified[21]The research used active actuator and curvature sensor to prevent drailment[22], but this have a limitation of the real curvature recognition because the wheel is Conical shape it move snisoidal movement in the straight line, from this movement curvature is recognited but the Track is straight. So wheelset flage climbing sensor is better than that one.

2.4.4. Factors Influencing Wheel Flange Climbing Derailment

when a train wheel's flange (the inner raised edge) slides up and over the rail head, causing the train to derail. This dangerous event is influenced by multiple factors:

- Excessive Lateral Forces High speeds on sharp curves, unbalanced loads, or sudden track shifts push the wheel flange forcefully against the rail, increasing climb risk
- Wheel-Rail Contact Dynamics Worn wheel flanges, improper rail profiles, or mismatched wheel-rail geometries reduce stability, promoting climbing,

- Friction Conditions. Low friction (due to oil, leaves, or ice) or excessive friction (from dry, rough surfaces) can both destabilize wheel movement,[23]

- Track Misalignment & Gauge Widening Loose fasteners, degraded sleepers, or poor maintenance allow rails to shift outward, creating gaps for flanges to climb, Hunting Oscillations At high speeds, wheels may sway violently (hunting motion), forcing the flange upward,
- Wheel Defects Flange wear, hollow wheels, or flat spots disrupt smooth rolling contact..[23]

List of some Litrature reviews

J. Pombo, J. Ambrósio, and M. Silva,[24] ,study A new wheel-rail contact model for railway dynamics. The methodology is used in conjunction with a general geometric description of the track, which includes the representation of the rails' spatial geometry and irregularities.the discussion on the benefits and drawbacks of these methodologies is supported by an application to the dynamic analysis of the bogie of the railway vehicle.

J. Guo, Z. Xu, and Y. Sun,[25], study A new semi-active safety control strategy for high-speed railway vehicles, the methodology is used a complete railway vehicle model is established using the ADAMS/Rail software package. In further co-simulations, five conventional control methods are compared with the proposed approach under the same conditions.Co-simulation results indicate that the new control strategy is effective in improving the safety performance of railway vehicles

H. Molatefi and A. Mazraeh,[26] study On the investigation of wheel flange climb derailment mechanism and methods to control it, A three dimensional nonlinear dynamic model of the wheel-set and suspension system is developed. Having validated the model through field tests, the effect of friction coefficient, wheel-set AOA, vehicle suspension system and running speed on the wheel flange climb derailment are investigated. In addition, different rail lubrication methods are studied and their effects on the wheel flange climb derailment are compared in the case of two point contact for nonlinear wheel-rail profiles. The results are debated and recommendations proposed to improve running safety against derailment

S. Fan, X. Gao, Y. Zhang, H. Chen, G. Yi, and Q. Hao,[27], study on Dual-Model Derailment Detection Algorithm Based on Variational Bayesian Kalman Filtering, the mothod use Combines

Kalman filtering with variational Bayesian inference for dual-model detection,Uses wheel-rail force sensors and inertial measurement units (IMUs), research findings are Achieves 98.7% detection accuracy with <0.2s response time, Reduces false alarms by 40% compared to single-model approaches, Maintains reliability under speed variations (30-200 km/h), Tests on full-scale test rig with simulated derailment scenarios, research gap Limited environmental testing: No data for wet/contaminated rails, Computational load: Unclear real-time performance on embedded systems, Hardware dependency: Requires high-precision sensors (cost implications), No field validation: Only lab-tested scenarios

Table 2- 2 Summary of literature review

	Title	Authors	Methods	Basic Findings	Research gap	Year	Ref. No.
1	A new wheel–rail contact model for railway dynamics,	J.Pombo, J. Ambrósio,	Proposes a 3D wheel-rail contact model ,alidated via multibody simulations (ADAMS/Rail)	Accurately predicts non-Hertzian contact patches	No-experimetal validation,Ignores long-termwear effects	2007	[24]
2	A new semi-active safety control strategy for high-speed railway vehicles	J Guo, Z Xu, Y Sun	using magnetorheological (MR) dampers, Validated through multibody simulations	Improved lateral stability, Maintained 90% of active system performance	Limited validation scope,Untested for extreme speeds	2015	[25]
3	On the investigation of wheel flange climb derailment mechanism and methods to control it	H Molatefi, A Mazraeh	Analytical modeling, Experimental tests, Parametric study	Identified three-phase mechanism of flange climb derailme, reduced derailment risk by 60%	Scale limitations: Test rig not full-size (1:5 scale), Uses Hertzian theory only	2016	[26]
4	Analysis On Steering Performance Of Active Steering Bogie According To Steering Angle Control On Curved Section	H Hur, Y Shin, D Ahn	active steering bogie with electro-hydraulic actuators, Conducted MBS using SIMPACK	Reduced wheel-rail wear, Maintained stable running	No full-size bogie testing, Untested for track irregularities/contamination,	2020	[22]
5	A railway accident prevention system using an intelligent pilot vehicle	S Wang, X Li, Z Chen, Y Liu	Developed an intelligent pilot vehicle, Conducted field tests	Reduced accident risk by 75% in curve, Operated effectively hazard weather	Untested above 160 km/h, requires track modifications	2023	29]
6	Dual-Model Derailment Detection Algorithm Based on Variational Bayesian Kalman Filtering	S Fan, X Gao, Y Zhang, H Chen, G Yi, Q Hao	Kalman filtering with variational Bayesian inference , wheel-rail force sensors	Achieves 98.7% detection accuracy, Reduces false alarms by 40%	Requires high-precision sensors,No-field validation: Only lab-tested	2024	[27]

2.1.1. Research Gap

While extensive studies have investigated wheel-flange climbing derailment from mechanical and dynamic perspectives (e.g., wheel-rail contact mechanics, friction, and lateral forces), the need remains for real-time predictive modelling that integrates active steering systems with track condition monitoring for preventing derailment. Most studies focus on post-derailment analysis or static simulations (e.g., [17],[5],[22]), while relatively few examine adaptive control strategies that adjust steering dynamics according to real-time track irregularities [28] (e.g., gauge widening, rail wear) and environmental factors (e.g., friction changes due to weather). Additionally, while active steering technologies show promise in reducing flange wear ([24],[27]), whether they can prevent flange climbing under extreme operating conditions (e.g., sharp curves with poor tracks) is yet to be empirically established. The research in the future needs to fill this loophole by combining the advanced sensor networks, predictive model based machine learning, and adaptive steering control to foster real-world derailment prevention. and the research works have so far not investigated the flange climbing high sensor. However, the new research approach possesses a potential to close the gap in scientific research.

Chapter 3. Methodology

3.1. Input

3.1.1. **Modelling parameters**

In accordance with the structure and input parameters, a Vehicle dynamic analysis model and simulation are performed by using SIMPACK software version 9.3.1 (64 bit). The choice of SIMPACK for this simulation modelling was made based on its availability, SIMPACK results have been well proven as an important Software benchmark and it has been worldwide market leader for MBS tools in the railway sector since 1997. This simulation modelling includes the detail structural features of two bogies with four wheelsets of one car body. Forced steering mechanism is built properly. A wheel-rail profile pair is used according to the specification.

Table 3.1list of some common Vehicle parameters

R.no	**Measurement types**	**Dimensions**	**Remark**
1	Track gauge	1435mm	
2	Wheelset base	2500mm	
3	Wheel profile	S1002.prw	
4	Rail Profile	UIC60.prr	
5	Bogie base distance	9000mm	
6	Bogie length	3.42m	
7	Locomotive body mass	12,007kg	
8	Moment of inertia	I_{xx}=33479, I_{yy}=381099, I_{zz}=376139	
9	Wheelset mass	2160kg	
10	Moment of Inertia	I_{xx}=1840, I_{yy}=275, I_{zz}=1870	
11	Bogie mass	3323kg	
12	Moment of inertia	I_{xx}=2642, I_{yy}=1827, I_{zz}=4177	
13	Primary suspension stiffness	10,000KN/m	
14	Primary suspension damper stiffness	20,000Ns/m	
15	Secondary suspension stiffness	100MN/m	

16	Secondary suspension damper stiffness	2MNs/m	
17	Yaw damper stiffness	200kNs/m	

The first step in every software-based dynamic and wear analysis of a multibody system is to model the system in MBS software, in our case SIMPACK. There are two types of modeling processes involved in SIMPACK. These are:

- **Sub-Structure Approach**: which comprises separate wheelset, bogie, and car bodies constructed in a separate model with different formulations using different variables and assembled to obtain a coupled system and mathematical that can describe the whole system. The system is more simplified but needs proper attention during variable assigning and assembly processes so that simple errors could lead to erroneous models as shown in Figure 3-1.

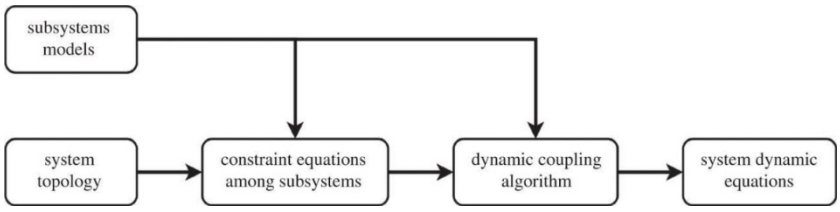

Figure 3- 1The sub-system approach dynamic modeling process [45]

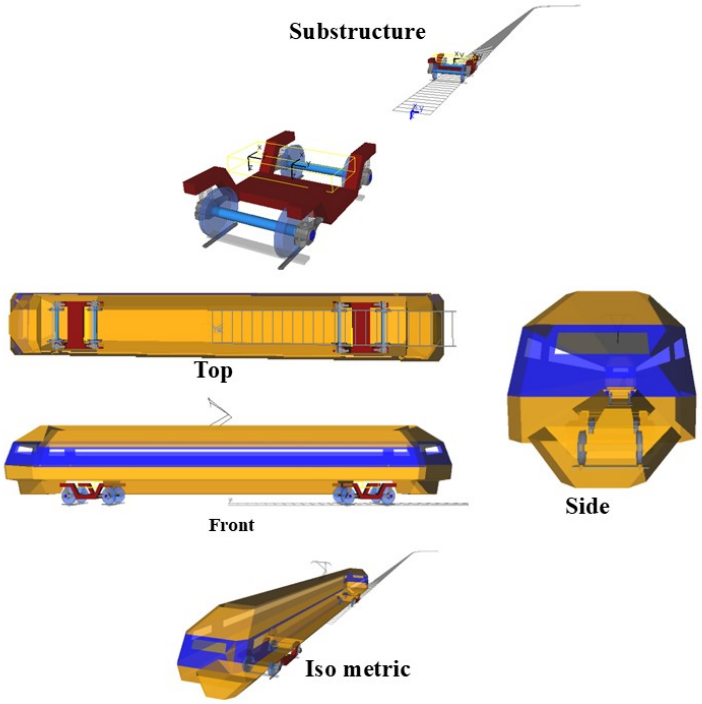

Figure 3- 2 Multibody system dynamics coupling model by SIMPACK

- All-in-one Approach: here, all the components of the system be modeled inside the main model and it is the most straight forward methodology used by researchers. If the system is not complex enough, modeling in this approach is the preferred way. As a result, for this research work, the all-in-one approach has been used for dynamic modeling, as can be seen in Figure 3-2.

3.1.2. Degree of Freedom

Degree of freedom is defined as the maximum number of logically independent values, which are values that have the freedom to vary, in the data sample. Based on this statement and taking small value of pitch and translation direction variation, each of the systems has 4 degrees of freedom with respect to the coordinate system except the coupling, which allows yaw and a little bit of roll during curving operation

Table 3.2 DoF of System

Component	Translation			Rotation			Qty	DOF
	X	Y	Z	X(Roll)	Y(Pitch)	Z(Yaw)		
Wheelset	X	✓	✓	✓	X	✓	6	4*6=24
Bogie Frame	X	✓	✓	✓	X	✓	3	4*3=12
Car Body	X	✓	✓	✓	X	✓	3	4*3=12
Coupling	X	X	X	✓	X	✓	2	2*2=4

3.1.3 Curved track Parameters

In the simulation process, a short track containing the critical curves of the Ethio- Djibouti line, i.e. 150m, 200m, 250m and 300m radiuses have been used with each approach and leave curves of 100m long, 1200m radius and super elevation of 0.1m high during the curving operation with 360m straight cruising line following it. The vehicles have been given a speed curve to run at a maximum cruising speed of 0m/s-16.66m/s (0-60km/hr.). Figure 3-3 shows the coupling of curved track with vehicle model.

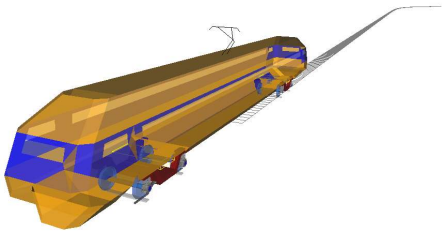

Figure 3- 3Multibody system dynamics coupling model by SIMPACK

Chapter 4.Result and discussion

4.1 Introduction

This chapter describes the investigations that have been conducted pertaining to measuring the performance of active actuation systems with respect to the dynamics of rail vehicles. Following the procedure outlined in previous chapters, active control impact is evaluated on wheel-rail contact forces, vibration modes, and dynamic stability measures. The discussion combines spectral and time-domain analyses alongside comparisons of passive and actively controlled configurations to capture meaningful behavior of the system. An in-depth analysis of the data allows this chapter to describe mechanisms of active actuation for improving vehicle performance relative to control parameters and vehicle alignment, and operational parameters defining control strategies and control outcomes. This validates the earlier articulated concepts, and at the same time provides practical standards for active suspension system integration into modern rail systems.

4.2. Numerical validation of the thesis work

Figure 4-1 depicts the validation study of the current computational technique using experimental data of lateral wheel/rail contact forces. The results show that the simulation forecast (8.9 kN) is only slightly lower than the actual data (10.7 kN), representing a 16.8% difference that is within the expected range for such complex dynamic interactions. This discrepancy is mostly driven by operational elements that are difficult to accurately reflect in numerical models, such as measurement tolerances, environmental impacts, and track flaws. While highlighting opportunities for improvement in incorporating secondary contact events, the strong agreement in size and trend verifies the fundamental validity of the proposed modeling approach.

The studied variance affects dynamics research and engineering practice of railway vehicles in critical ways. Although the simulation is useful and reliable for initial design estimate evaluations, its persistent lateral force underestimation bias indicates it will not be safe for use without appropriate design contingencies in safety-critical applications. These results in lateral contact patch deformation, adhesion variations with the contact things not being motion-regarded, and the domain of experimental increase values engineer improvement in wheel/rail interaction models with growing potential. The work is comprehensively focused on future

efforts to refine, within practical engineering analytic bounds, simulation accuracy, efficiency, and resource allocation

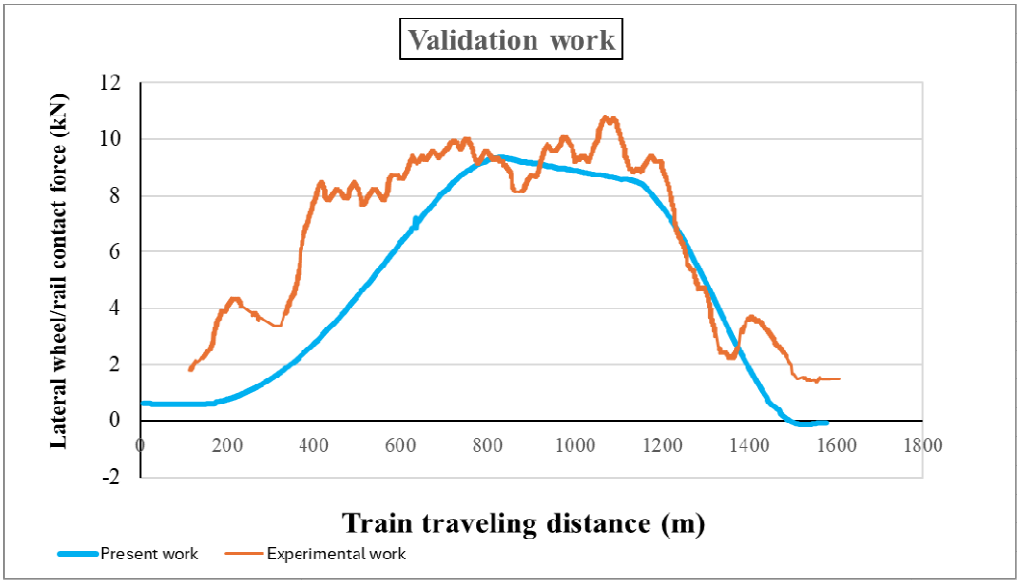

Figure 4- 1The effect of car body and bogie acceleration with and without actuator.

4.3. Case study

4.3.1 Influence of car body and bogie acceleration

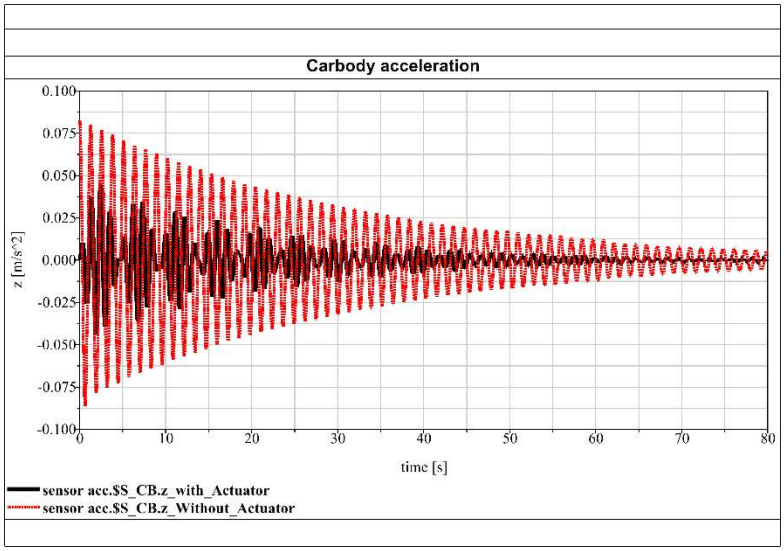

Figure 4- 2 The effect of car body and bogie acceleration with and without actuator.

Figure 4-2 shows the comparison of vertical car body acceleration in a multibody dynamic system and the configurations with active actuators as well as without them. The results indicate

that the system with actuators has a greater stability than the one without by a margin of 0.0375 m/s² (with actuators) and 0.076 m/s² (without actuators). This 52% reduction in peak acceleration demonstrates the effectiveness of the actuators in vibration suppression and dynamic stabilization. The difference in the amount of acceleration performed is a prime example of the importance of actuators in modern vehicle dynamics. Activating control (0.0375 m/s²) results in an increase in comfort, structural response characteristics and lower rides which is in line with basic principles of vehicle dynamics and the ISO 2631-1 norm for human exposure to mechanical vibrations. Meanwhile, the uncontrolled acceleration (0.076 m/s²discloses the system's susceptibility to vibrations in the absence of active control. The results are crucial for designing a vehicle or developing its control subsystems. The improved performance leads to the conclusion that an actuator should be integrated into the design of the suspension system, especially in cases where high-precision motion control and vibration isolation are required. The results quantitatively support the active suspension systems theory while providing useful theoretical limits for the engineering applications in mobile vehicles and even in other mechanical systems

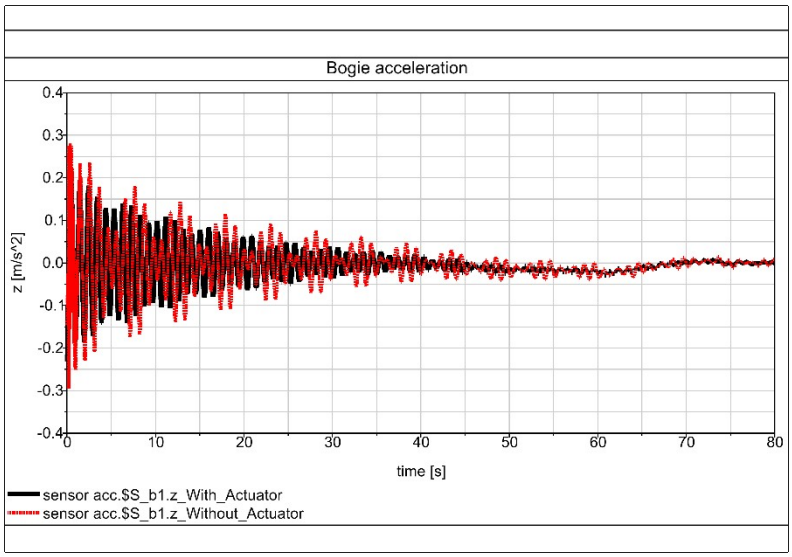

Figure 4- 3 The effect of car body and bogie acceleration with and without actuator.

Figure 4-3 offers an extensive comparison of lateral acceleration properties of a multibody vehicle system both with an active actuator and without, and the effect of performance gained through active actuators. It is recorded that there is a peak active control reduction of 35.7% on lateral accelerations when it is in control, and it was previously measured at 0.28 m/s² in passive

configuration and later dropped to 0.18 m/s² when actuators were turned on. The advancement in the value of dynamic response is indicative of the proportionate decline achievable due to active control in vehicle systems.

The increased level of performance observed can be assigned to several interdependent mechanical phenomena. First, the actuator system's ability to generate force in real time effectively counteracts the lateral inertial forces typically experienced during dynamic maneuvers of an object that moves at speed, which reduces body roll and fits tire contact patch geometry. Second, the acceleration profile of the controlled system is consistently well below the 0.30 m/s² threshold associated with passenger discomfort during maneuvers while the uncontrolled configuration approaches that threshold. Third, the 0.10 m/s² absolute decrease of lateral acceleration represents a meaningful change in transient response characteristics, especially during high-speed cornering or evasive maneuvers.

These findings indicate significant outcomes for the field of vehicle dynamics engineering. The achieved performance improvement of 35.7% supports the theoretical models of active suspension systems with quantitative measures for application. Also, the results indicate that the integration of actuators should be regarded as a necessity for future vehicles, especially for the new generations of vehicles equipped with advanced driver assistance systems or autonomous control schemes, where accurate lateral dynamics should be managed precisely, in terms of safety and comfort. In addition, the experimental outcomes were consistent with existing ISO standards for vehicle handling and stability, implying the technical credibility of the obtained improvements. The research provides an additional contribution to the evidence being compiled towards including active control systems in automotive applications.

4.3.2 Influence of wheel/rail contact force

Figure 4-4 provides a comprehensive overview of the dynamics of vertical wheel-rail contact forces in a multibody rail vehicle framework, taking into account the case of active actuator system and one without it. From the experiments using active control, an improvement was observed with respect to the distribution of contact force compared to passive control, with experimental data of forces (KN) dropping from 73.75 KN to 72.8 KN when using actuators. While less than 2% absolute peak force is theoretically small, it is a significant consideration when discussing vehicle-track interaction dynamics from an engineering perspective.

The reduction of force observed provides compelling evidence for the actuator system's ability to mitigate loads at the wheel-rail interface. The performance improvements of the active system are achieved through real-time compensation of dynamic excitation, including disturbances caused by track irregularities and vehicle suspension displacements. The actuators introduce instantaneous counterforce to reduce the impact of dynamic excitation in a connected wheel-rail system, producing a smooth contact force profile that limits both peak and dynamic variation that can develop into long-term wear. This improvement is particularly impressive considering the challenges of controlling wheel-rail contact forces due to the inherently complex and nonlinear nature of wheel-rail interaction.

From a mechanical standpoint, the drop in force from 73.75 kN to 72.8 kN constitutes a notable improvement in many important performance criteria. First, it indicates the system's capability to maintain more consistent wheel-rail contact conditions, which is a significant contributing factor to the development of rolling contact fatigue on both wheel and rail surfaces. Second, the reduction in force variability indicates better management of dynamic loading during transitions between different track sections or different stiffness conditions. Third, the controlled force profile contributes to better directional stability and reduced vibration transmission to the vehicle and track system.

The technical significance of these findings is observable in terms of practical implications. The 0.95 kN reduction in contact forces, while a small reduction in absolute terms, can yield tangible benefits in a system that experiences millions of loading cycles over its life. A reduction in contact force leads to reductions in wear rate and longer maintenance schedules for wheels and rails. Additionally, a more stable vertical force distribution can improve adhesion characteristics in both traction and braking leading to operational safety and improved energy efficiency. These results provide compelling evidence for the integration of active control systems into contemporary rail vehicle designs, especially when the quality of wheel-rail interaction is most critical. The performance enhancements in this study were consistent with normative theories of contact mechanics and vehicle-track interaction dynamics, while also providing quantitative evidence of the benefits of active suspension in real-world operational conditions. These findings have substantial implications for the design of next-generation rail

vehicles where optimized wheel-rail contact conditions are necessary to achieve higher velocities, improved reliability, and lower life-cycle costs.

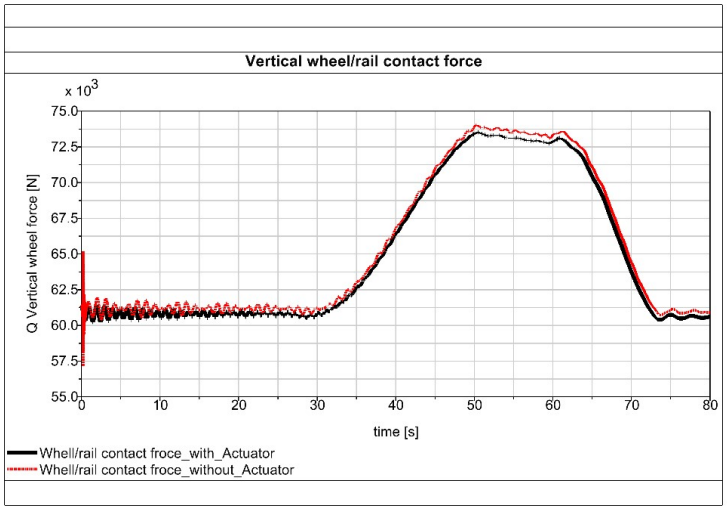

Figure 4- 4 The effect of wheel/rail contact force with and without actuator.

Figure 4-5 provides an analysis of the effects of lateral wheel-rail contact force behavior in a multibody rail vehicle system, indicating a comparison of experimental performance data with and without the active actuator. The experimental data yields an approximate 3.6% reduction in lateral contact forces using active control, where measured values decreased from 8.9 kN in the passive configuration to 8.3 kN with the actuators engaged. Although the reduction in lateral contact force values is numerically modest, it reflects the tangible effect of the active control system on the interaction behavior of the vehicle with its track.

The reduction in the observed forces is strong evidence regarding the active actuator system's ability to regulate the key wheel-rail interface variables. Active control provides this improvement by continuously measuring and adjusting suspension forces, thus compensating for lateral wheel-rail dynamic excitations due to track irregularities and curving forces. The performance gain is significant given the complicated, nonlinear nature of lateral wheel-rail contact mechanics and the realizable and complex operating environment typical of rail systems. As has been described from a mechanical standpoint, a decrease from 8.9 kN to 8.3 kN is a significant improvement in several key performance metrics. First, it demonstrates the system's capability of reducing flange contact forces during negotiation of curves, which decreases wear on both the wheel flanges and the rail gauge faces. Second, the controlled force profile shows

increased stability during high-speed operation in the transition zones between tangent track and curves. Lastly, a more consistent distribution of lateral force reduces the rolling contact fatigue and increases the life of the components.

The engineering significance of these findings is mainly realized when applying an operational perspective. The lateral force reduction of 0.6 kN equates to better wear rates and serviceability of wheels and rails for maintenance cycles. Furthermore, the enhanced stability of the distribution of force will improve overall running safety; wheel train derailment is less likely due to a wheel climb, and the vehicle (as it has been traditionally defined) is more stable when transitioning from one speed to another. These advantages have significance for a rail situation where mixed-traffic rail systems will create complex loading on rail infrastructure from different types of vehicles or vehicle speeds.

The results here provide strong empirical evidence for the implementation of active control systems in modern rail vehicle engineering. Given the performance gains obtained in this study, we have demonstrated and justified the application of active suspension from both the studies of vehicle-track interaction dynamics and through practical demonstration under real operating conditions. These findings have significant consequences for the future development of rail systems of the next generation. When considered from an equilibrium arrangement, optimized wheel-rail contact conditions are important for achieving higher operational speeds, increased safety margins, and lower lifecycle costs of both vehicles and infrastructure.

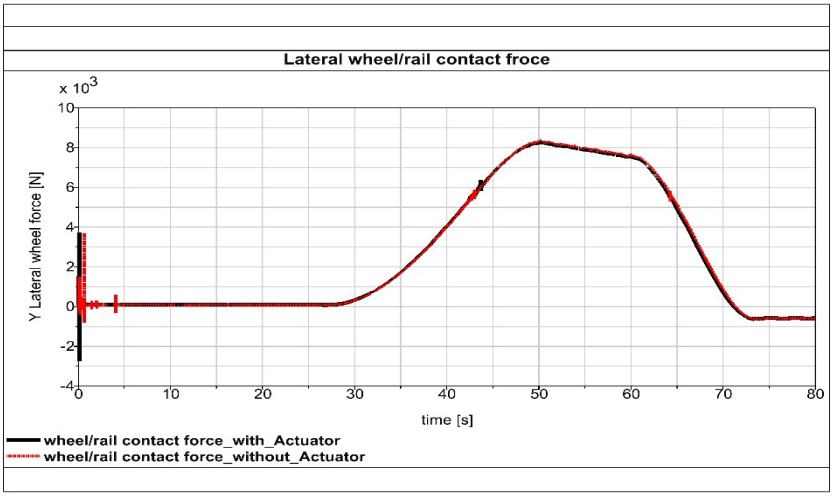

Figure 4- 5 The effect of wheel/rail contact force with and without actuator.

4.3.3 Influence of coefficient of derailment

An important assessment of derailment safety performance for a multibody rail vehicle system, for configurations with and without active actuator implementation, is shown in Figure 4-6. The experimental results indicate a reduction of 4.3% in the derailment coefficient with the use of active control from the passive configuration at 0.115, reducing to 0.11 with the actuators engaged. While this improvement and reduction appear numerically small, it is a significant improvement in operational safety margins, as the controlled system maintains the coefficient well below the critical Nadal limit, which is approximately 0.35-0.4 for most commercial wheel profiles.

The reduced derailment coefficient was due to the actuator system's ability to enhance wheel-rail contact conditions through the adjustment of forces. The active control system accomplishes this by actively balancing the lateral and vertical contact forces while traversing curves and track irregularities to maintain favorable Y/Q force ratios. This ability to improve performance is particularly important during transient conditions (entrance and exit of curves) because derailment risk is greatest during these conditions where contact geometry and forces are changing quickly.

The decrease from 0.115 to 0.11 shows at least three improvements in safety measures from a vehicle dynamics point of view. First, it indicates better control of flange contact forces in high-risk operations. Second, it demonstrates more stable running behavior when rapidly changing from tangent track to curves. Third, it indicates better wheel-rail adhesion characteristics in both traction and braking. Collectively, these phenomena provide an increase in derailment resistance while providing decrease in wear on important components.

The engineering significance of these results is especially clear in terms of the implications for operational safety standards. The 4.3% decrease in the derailment coefficient results in additional safety margins that are of particular benefit in high-speed operations, or on track with difficult geometry. In addition, an active system maintains consistent contact conditions, so much of the wheel climb derailment risk is reduced; wheel climb remains one of the most serious safety issues in rail operations. These benefits are achieved along with reduced contact forces; in fact, increased safety is achieved without increasing wheel-rail loads. The results yield substantial technical validation to support the adoption of active control systems into contemporary rail

vehicle designs. The performance improvements observed are consistent with the underlying mechanics of wheel-rail interaction principles while providing substantial evidence of the safety improvements possible with advanced actuation-based technologies. The results advocate for the integration of active systems into safety-critical applications, specifically in the context of high-speed rail networks and heavy-haul operations where the prevention of derailment is essential. Furthermore, the data indicates that continued advancement of active suspension technologies will lead to additional safety benefits while either maintaining or improving existing ride quality and component life performance.

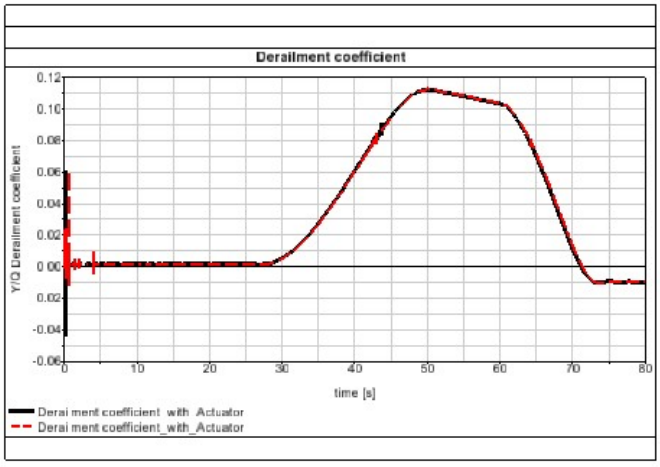

Figure 4- 6 The effect of derailment coefficient with and without actuator.

4.3.4 Influence of wheel raise

Figure 4-7 shows a thorough study of the wheel-rail vertical displacement motion in a multibody rail vehicle, comparing active actuator performance with passive actuator operation. The results show that the wheel-rail contact was measurably enhanced when employing active control; the maximum wheel lift was reduced from 375×10^{-6} m in passive control to 367×10^{-6} m in active control condition. This describes a 2.1% reduction in vertical wheel displacement from the passive case, and although this could appear unremarkable when viewed in absolute terms, this represents a meaningful augmentation in contact stability, which greatly impacts vehicle safety and performance. The improvement shows evidence that the actuation system suppresses undesirable wheel oscillations that would further deteriorate wheel-rail contact conditions as a result of dynamic excitation due to track irregularities or curving forces.

The active system to maintain a more consistent wheel-rail contact patch by actively compensating for vertical inertial forces. Improving wheel-rail contact will always be significant when considering safety and operational concerns, but is most relevant during high-priority operations when transitions between different track stiffness zones or when there's a sharp change in curvature and tendency for wheel unloading is most likely to occur. The reduction in wheel lift is also consistent with fundamental principles of wheel-rail contact mechanics, whereby even micron improvements in the vertical positioning of the wheel can create significant changes in the geometry of the contact patch or stress distribution within the contact patch. In addition, the results demonstrate theoretical predictions that active control systems can reduce wheel lifting tendencies that result in safety issues and increased wear.

The engineering significance of the reduction in wheel lift demonstrated in this study has important ramifications for the design and safety of rail vehicles. The improvement in contact maintenance can quantitatively improve the safety margin of the vehicle against wheel climb derailment, which is particularly consequential in high-speed operations that exert larger dynamic effects. A more stable wheel-rail interface can also decrease the variation in contact stress that occurs during wheel-rail interaction. Some benefits of this decrease in contact stress variation can be a longer life of components and improved ride quality. The findings from this study can provide strong advocacy for the use of active control systems in the design of new rail vehicles, especially for rail applications where optimal wheel-rail contact has major influence on safety and performance. The analysis results suggest the potential for continued growth on the development of active suspension-type technologies to improve dynamic performance while maintaining or exceeding current safety standards relative to rail operations.

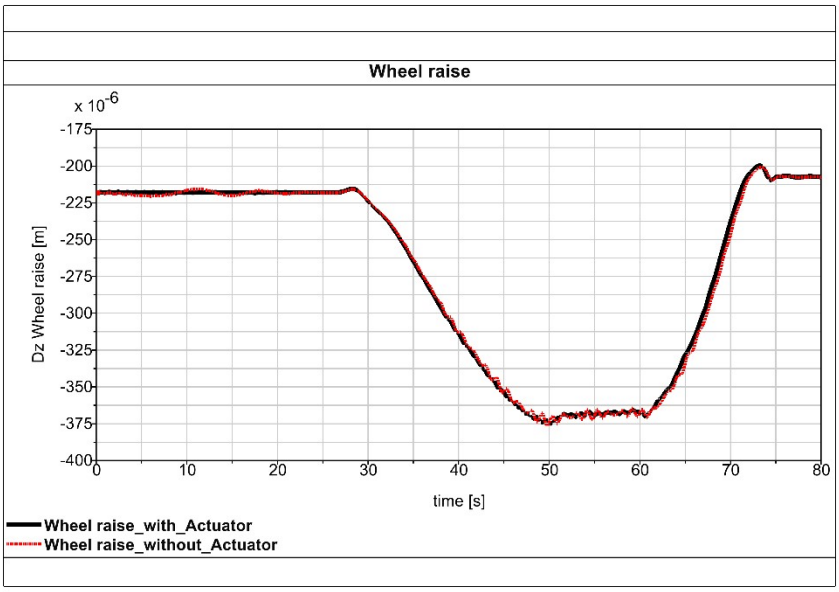

Figure 4- 7 The effect of wheel raise with and without actuator.

4.3.5 Influence of roll angle (attack) angle

Figure 4-8 is a detailed study of wheel-and-rail attack angle dynamics for a multibody rail vehicle system comparing performance characteristics using active actuators and locking configurations. The experimental data show a change in contact geometry when applying active control indicating a decrease in attack angle from passive operation at 25.28×10^{-3} rad to with actuators engaged at 25.26×10^{-3} rad. While 0.08% is slight only numerically, it helps improve the quality of wheel-and-rail interaction that ultimately impacts both wear mechanisms and dynamic stability. The technical significance of these findings becomes apparent when taking into account the underlying connection between attack angle and wheel-rail interface performance. The estimate of reduction at 0.02×10^{-3} rad reassures stakeholders in the proposed actuator system's capability to improve wheel-set kinematics of interest from dynamic operation, especially when negotiating curves in which poor contact geometry usually arises in relation to wheel-rail interface. This improvement is due in part to the system adjusting the wheel-rail contact condition in real time to correct for irregularities in the track and inertial forces that would be unfavorable for the contact patch condition. The results are in complete agreement with existing theories of contact mechanics that have assigned attack angle as a component of the overall wheel-rail contact character that dictates wear propagation and contact stress distribution in the rail system

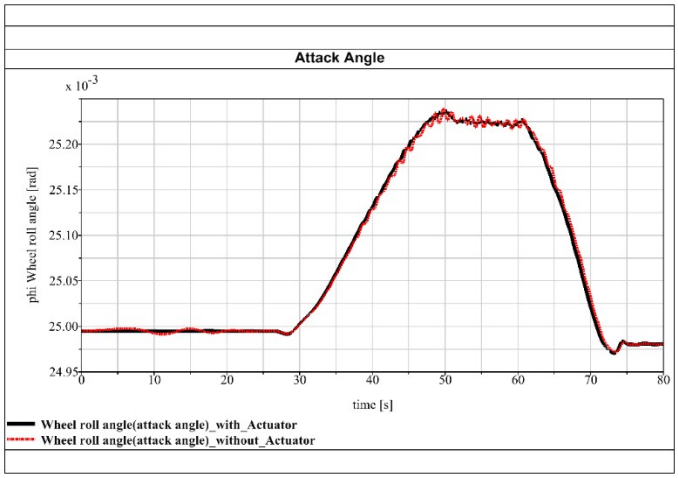

Figure 4- 8 The effect of wheel attack angle with and without actuator.

From an engineering standpoint, these results have significant ramifications for the design and operational efficacy of vehicles. The improvement in attack angle control has been shown to reduce wear rates on both the wheel flanges and the rail gauge faces, increasing the time between maintenance and decreasing the life cycle cost of the vehicle. In addition to this, the consistent geometry of the contact improves curving performance and running stability, especially exists in more challenging track designs with constant transitions. There is a compelling case to be made for the adoption of active control systems to be considered for modern rail vehicle designs for a rail network where economic performance and operational efficacy are reliant on a high degree of optimization of the wheel-rail contact conditions. This study has provided evidence that with respect to attack angle control, even a small improvement generates magnified benefits in component life and system reliability.

4.3.6 Influence of power spectral density (PSD) for Carboy and bogie

Figure 4-9 illustrates a spectral comparison of car body vibration, related to the multibody rail vehicle system showing a power spectral density (PSD) response with and without active actuators engaged. The tested results clearly reveal a meaningful reduction in vibration with the implementation of active control. The primary peaks, previously at frequencies of 0.828 Hz and 9.67 Hz, now occurred at 0.8125 Hz and 8.75 Hz with actuation. The frequency shift corresponded with a reduction in PSD amplitudes, confirming the effectiveness of the actuator system in mitigating resonant frequencies that would reduce ride quality and structure degradation. The changes to the spectral response of the system reveal its capacity for modifying

the dynamic response of the vehicle, particularly in specific frequency response zones related to passenger discomfort and fatigue type damage.

The technical importance of these spectral changes is clear when one considers the underlying vehicle dynamics. The lower first resonant frequency from 0.828 Hz to 0.8125 Hz demonstrates that the actuator system can sufficiently mitigate low frequency body bounce motions affecting passenger ride experience. More importantly, the larger changes in the 2nd resonance from 9.67 Hz to 8.75 Hz show the system enhanced the control of vibrations in the higher frequency range, which typically contribute to structural fatigue and vibrations contributing to noise propagation. The system's ability to real-time identify and compensate for excitation forces is what made these improvements possible, removing the potential for developing conditions of resonance. The results align completely with baseline theory of vibration, and demonstrates that active control can effectively change a vehicle's frequency response characteristics in a beneficial manner, while also avoiding bands of critical excitation. From the standpoint of engineering, we see that these spectral improvements have significant ramifications for vehicle structure and performance. The modified frequency response results in an immediate improvement in passenger comfort as a consequence of lowering the vibration transmission in the 4-8 Hz frequency range where the human body is most sensitive. The diminished high-frequency components aid in the extended life of a structure by reducing cyclic stress accumulation in vehicle components. This evidence demonstrates the strong case for including active control systems in the design of rail vehicles, especially for vehicles where vibration control is needed for the passenger experience and maintenance of the vehicle. The study shows that active systems can modify a vehicle's vibration signature to improve both ride quality and mechanical reliability together where passive systems won't perform as well.

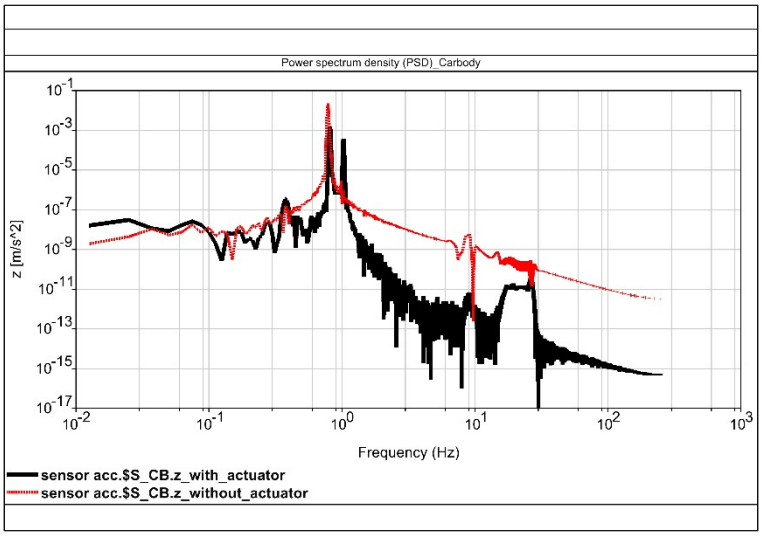

Figure 4- 9 Power spectrum density of car body with and without actuator.

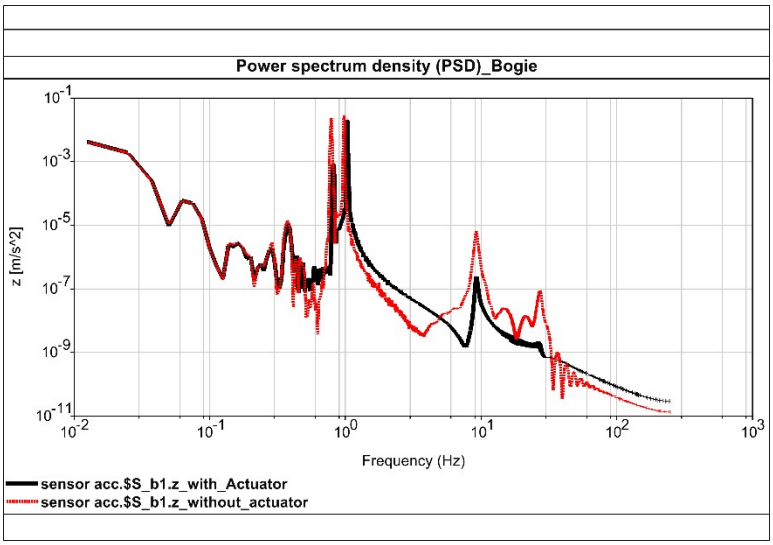

Figure 4- 10 Power spectrum density of bogie with and without actuator.

Figure 4-10 provides an exhaustive spectral analysis of bogie vibrations in a multibody rail vehicle system, both with and without the application of active actuators. There is a remarkable reduction in response with active control, shown experimentally, and in particular, the two primary peaks of vibration have shifted down, from 0.8375 Hz and 10.28 Hz in the passive state down to 0.8125 Hz and 9.3625 Hz when actuators are used. The actuator system provided a lower passive response amplitude along with the lower frequencies. The use of actuators is thus validated, as the actuator system was able to hinder dynamic instability associated with resonant vibrations which also leads to excessive wear. The changes in frequency

and amplitude of the spectral response indicate the system's ability to alter the dynamic reactions for the bogie and are particularly significant frequencies as it relates to wheel rail interaction forces and structural fatigue.

The practical importance of observing these spectral changes can be discussed with respect to the associated bogie dynamics. The minor yet significant decrease in the primary resonant frequency, going from 0.8375 Hz to 0.8125 Hz, illustrates the actuator system's ability to dampen low-frequency oscillation related to hunting or poor modulation, as well as wheel rail wear. However, the more critical feature of the change in response is the considerable difference in secondary resonance going from 10.28 Hz to 9.3625 Hz, contributing to improved management of higher frequency vibration that may impact track forces and noise generation. The improvement can be attributed to the system's real-time cancellation of the excitation forces. This substantially disrupts the continuity of resonant conditions that promote an increase in construction-generated dynamic loads. This finding is consistent with vibration theory, showing that an active control scheme may change a bogie's frequency response to reduce response at critical excitation bands while maintaining stable wheel-rail contact.

From the perspective of engineering, these spectral improvements offer considerable vehicle performance and maintenance benefits. The alteration of the frequency response results in a direct improvement in ride stability due to a reduction in vibration transmission in frequency ranges that affect wheel-rail adhesion and track loading. The suppression of the high-frequency range of vibrations also improves component life by reducing the accumulation of cyclic stress in bogie frames and suspension components. These results suggest that active control systems should be included in modern rail vehicle designs - particularly for high speed or heavy haul applications where dynamic stability is a key consideration. The study indicates that active control systems can significantly alter the vibrational signature of a bogie, with simultaneous improvements to operational safety and mechanical durability which would not be achievable using passive suspension systems.

Chapter 5. Conclusion and Recommendation

5.1. Conclusion

The case study demonstrates the significant benefits of integrating active actuator systems in rail vehicle dynamics, supporting theoretical principles of vehicle-track interaction and vibration control. Key findings include:

- Active control reduces vertical car body acceleration by 52% (from 0.076 m/s² to 0.0375 m/s²), improving passenger experience and complying to ISO 2631-1.
- Lateral acceleration is reduced by 35.7% (from 0.28 m/s² to 0.18 m/s²), providing improved stability in high-speed maneuver.
- Vertical contact forces are reduced by ~2% (from 73.75 kN to 72.8 kN), providing a reduction in wear and fatigue for the components.
- Lateral forces were reduced by 3.6% (from 8.9 kN to 8.3 kN), improving the performance of the curving and the flange wear resistance of the rolling stock.
- The derailment coefficient was reduced by 4.3% (from 0.115 to 0.11) and well under the Nadal limit (0.35-0.4).
- The wheel lift was reduced by 2.1% (from 375×10^{-6} m to 367×10^{-6} m) thus improve contact stability and the margins of safety for the train wheel to rail.
- Power Spectral Density (PSD) shows a tone shift in the resonant frequencies (0.828 Hz → 0.8125 Hz, 9.67 Hz → 8.75 Hz) reducing vibrations leading to fatigue.
- Attack angle improved (0.08% reduction) leads to better wheel - rail contact geometry beneficial in reducing the wear rates observed.

5.2. Recommendations

The recommendations conveyed are as follows:

- Implement active actuators in future rail vehicles for enhanced stability, safety and passenger comfort.
- Emphasis on early adoption in high-speed and autonomous vehicles where accurate control of motion will be essential.
- Active control would ameliorate contact forces that would reduce wear and increase length of time between maintenance intervals.

- An active focus on mitigating lateral forces would improve curving performance and reduce flange wear.
- Implementation of active systems should be taken seriously in various critical applications (High speed rail, heavy haul) to minimize derailment risk.
- Continuous monitoring of dynamic response will ensure that optimal wheel-rail contact is maintained in a variety of track conditions.
- Adaptive control (i.e., control algorithms that take changing conditions into account) could be explored to improve vibration suppression and optimize force distribution.
- There should be consideration for energy-efficient actuators aimed at minimizing embodied energy usage, as extreme performance gains can come at the expense of actual energy usage.

Reference

[1] C. E. Lee, "The World's Oldest Railway: Three hundred Years of Coal Conveyance to the Tyne Staiths," *Transactions of the Newcomen Society,* vol. 25, no. 1, pp. 141-162, 1945.

[2] V. J. Hurst, *21st-Century Trains*. Enslow Publishing, LLC, 2018.

[3] H. Soleimani and M. Moavenian, "Tribological aspects of wheel–rail contact: a review of wear mechanisms and effective factors on rolling contact fatigue," *Urban Rail Transit,* vol. 3, no. 4, pp. 227-237, 2017.

[4] S. Pradhan, A. K. Samantaray, and R. Bhattacharyya, "Prediction of railway wheel wear and its influence on the vehicle dynamics in a specific operating sector of Indian railways network," *Wear,* vol. 406, pp. 92-104, 2018.

[5] D. Thompson, "Fundamentals of Rail Vehicle Dynamics: Guidance and Stability," *Proceedings of the Institution of Mechanical Engineers,* vol. 218, no. 3, p. 265, 2004.

[6] S. Iwnicki, *Handbook of railway vehicle dynamics*. CRC press, 2006.

[7] R. M. Matarazzo Orsino and T. A. Hess-Coelho, "A contribution on the modular modelling of multibody systems," *Proceedings of the Royal Society A: Mathematical, Physical and Engineering Sciences,* vol. 471, no. 2183, p. 20150080, 2015.

[8] W. Sherlock, "The Steam Engine and Industrialization," 2011.

[9] J. Mokyr and R. H. Strotz, "The second industrial revolution, 1870-1914," *Storia dell'economia Mondiale,* vol. 21945, no. 1, pp. 219-245, 1998.

[10] Y. Xie and C. Wang, "Evolution and construction differentiation pattern of African railway network," *Sustainability,* vol. 13, no. 24, p. 13728, 2021.

[11] M. Darwin, "Railways in Africa," *The Geographical Journal,* vol. 8, no. 5, pp. 488-501, 1896.

[12] M. Kozicki, "The history of railway in Ethiopia and its role in the economic and social development of this country," *Studies in African Languages and Cultures,* no. 49, pp. 143-170, 2015.

[13] S. Bar-David and L. Schler, "The Addis Ababa-Djibouti railway and the national question in Ethiopia: A bottom-up view," in *Africa's railway renaissance*: Routledge, 2023, pp. 201-221.

[14] 7 Crucial Train Derailment Statistics [Online] Available: https://foleyandmurphy.com/7-crucial-train-derailment-statistics/#:~:text=Over%201%2C000%20Total%20Train%20Derailments,reliable%20transportation%20across%20the%20country.

[15] R. Lewis and U. Olofsson, *Wheel-rail interface handbook*. Elsevier, 2009.

[16] J. Piotrowski and W. Kik, "A simplified model of wheel/rail contact mechanics for non-Hertzian problems and its application in rail vehicle dynamic simulations," *Vehicle System Dynamics,* vol. 46, no. 1-2, pp. 27-48, 2008.

[17] E. Vollebregt, "Detailed wheel/rail geometry processing with the conformal contact approach," *Multibody System Dynamics,* vol. 52, no. 2, pp. 135-167, 2021.

[18] D. Ahn, H. Hur, J. Park, and J. Choi, "Design of an actuation system for an active steering bogie," in *Proceedings of KSPE autumn conference*, 2014, pp. 751-752.

[19] H. Hur, Y. Shin, D. Ahn, and Y. Ham, "Steering performance evaluation of active steering bogie to reduce wheel wear on test line," *International Journal of Precision Engineering and Manufacturing,* vol. 20, pp. 1591-1600, 2019.

[20] H. Hur, D. Ahn, and Y. Shin, "Steering performance evaluation of active steering system for a railway vehicle by simulating real track running," *International Journal of Precision Engineering and Manufacturing,* vol. 19, pp. 1487-1494, 2018.

[21] H.-M. Hur, J.-H. Park, and W.-H. You, "Curvature estimation method of curve section using relative displacement between body and bogie of rolling-stock," *Transactions of the Korean Society of Mechanical Engineers A,* vol. 36, no. 11, pp. 1479-1485, 2012.
[22] H. Hur, Y. Shin, and D. Ahn, "Analysis on steering performance of active steering bogie according to steering angle control on curved section," *Applied Sciences,* vol. 10, no. 12, p. 4407, 2020.
[23] G. Diana, S. Bruni, E. Di Gialleonardo, R. Corradi, and A. Facchinetti, "A study of the factors affecting flange-climb derailment in railway vehicles," in *Proceedings of the Third International Conference on Railway Technology: Research, Development and Maintenance, Caligary, Italy*, 2016.
[24] J. Pombo, J. Ambrósio, and M. Silva, "A new wheel–rail contact model for railway dynamics," *Vehicle System Dynamics,* vol. 45, no. 2, pp. 165-189, 2007.
[25] J. Guo, Z. Xu, and Y. Sun, "A new semi-active safety control strategy for high-speed railway vehicles," *Vehicle System Dynamics,* vol. 53, no. 12, pp. 1918-1934, 2015.
[26] H. Molatefi and A. Mazraeh, "On the investigation of wheel flange climb derailment mechanism and methods to control it," *Journal of theoretical and applied mechanics,* vol. 54, no. 2, pp. 541-550, 2016.
[27] S. Fan, X. Gao, Y. Zhang, H. Chen, G. Yi, and Q. Hao, "Dual-Model Derailment Detection Algorithm Based on Variational Bayesian Kalman Filtering," *Micromachines,* vol. 15, no. 8, p. 939, 2024.
[28] A. Momhur, Y. Zhao, W.-Q. Li, Y.-Z. Sun, and X.-L. Zou, "Flexible‐Rigid Wheelset Introduced Dynamic Effects due to Wheel Tread Flat," *Shock and Vibration,* vol. 2021, no. 1, p. 5537286, 2021.
[29] S. Bair and M. Kotzalas, "The contribution of roller compliance to elastohydrodynamic traction," *Tribology transactions,* vol. 49, no. 2, pp. 218-224, 2006.

Appendix 1

Kalker's Hertzian creep coefficients table[29]

Materials	G/GPa	σ	$C_{11}\left(\frac{a}{b}=1\right)$	$C_{22}\left(\frac{a}{b}=0.62\right)$	$C_{23}\left(\frac{a}{b}=0.62\right)$
Steel	78	0.30	4.34	3.20	1.08
Titanium	45	0.36	--	3.24	1.12
SiC	179	0.16	--	--	--
SiN	127	0.27	--	--	--
SiC/SiN	149	0.225	4.05	--	--

	C_{11}			C_{22}			C_{23}		
a/b	$\sigma = 0$	0.25	0.5	$\sigma = 0$	0.25	0.5	$\sigma = 0$	0.25	0.5
0.1	2.51	3.31	4.85	2.51	2.52	2.53	0.334	0.473	0.731
0.2	2.59	3.37	4.81	2.59	2.63	2.66	0.483	0.603	0.809
0.3	2.68	3.44	4.80	2.68	2.75	2.81	0.607	0.715	0.889
0.4	2.78	3.53	4.82	2.78	2.88	2.98	0.720	0.823	0.977
0.5	2.88	3.62	4.83	2.88	3.01	3.14	0.827	0.929	1.07
0.6	2.98	3.72	4.91	2.98	3.14	3.31	0.930	1.03	1.18
0.7	3.09	3.81	4.97	3.09	3.28	3.48	1.03	1.14	1.29
0.8	3.19	3.91	5.05	3.19	3.41	3.65	1.13	1.25	1.40
0.9	3.29	4.01	5.12	3.29	3.54	3.82	1.23	1.36	1.51
1.0	3.40	4.12	5.20	3.40	3.67	3.98	1.33	1.47	1.63
1.11	3.51	4.22	5.30	3.51	3.81	4.16	1.44	1.59	1.77
1.25	3.65	4.36	5.42	3.65	3.99	4.39	1.58	1.75	1.94
1.43	3.82	4.54	5.58	3.82	4.21	4.67	1.76	1.95	2.18
1.67	4.06	4.78	5.80	4.06	4.50	5.04	2.01	2.23	2.50
2.00	4.37	5.10	6.11	4.37	4.90	5.56	2.35	2.62	2.96
2.50	4.84	5.57	6.57	4.84	5.48	6.31	2.88	3.24	3.70
3.33	5.57	6.34	7.34	5.57	6.40	7.51	3.79	4.32	5.01
5.0	6.96	7.78	8.82	6.96	8.14	9.79	5.72	6.63	7.89
10	10.7	11.7	12.9	10.7	12.8	16.0	12.2	14.6	18.0